

# Supporting Information: DICE: A Monte Carlo code for molecular simulation including Configurational Bias Monte Carlo method

Henrique Musseli Cezar\*, Sylvio Canuto†, Kaline Coutinho‡

Universidade de Sao Paulo, Instituto de Fisica, 05508-090, Sao Paulo, SP, Brazil

## SI 1: DICE implementation and features

### SI 1.1: Overview

DICE is a software for the simulation of gases and liquids using Monte Carlo methods, as described in main text, written in Fortran using OpenMP for a shared memory parallelization. This code is available at <https://portal.if.usp.br/dice>. The units of the variables are: kcal/mol for energy, Å for distance and positions, K for temperature, atm for pressure, g/cm<sup>3</sup> for density,  $e$  for charge, ° for angles and kcal/(mol Å<sup>2</sup>) and kcal/(mol rad<sup>2</sup>) for spring constants for the bonds and angles, respectively. DICE uses the Mersenne Twister pseudo random number generator,[1] specifically, the implementation by Tsuyoshi Tada.[2] Along this text, important input keywords will be presented in parenthesis. The current version of the software is able to do simulations in the *NVT* (`vstep = 0`) and *NPT* ensembles, in periodic boxes with two shapes: cubic (`geom = 0`, default) or parallelepiped (`geom = 1`). The initial configuration can be read or randomly generated, with the minimum distance between atoms defined by the user (`rmin_ini = 1.5`, default). During the run, the state of the simulation is saved periodically (`isave = 1000`, default), so the user may continue (`accum = yes`) a simulation.

A simple Verlet neighbor list is used to reduce computational cost.[3] In this scheme, additionally to the usual cutoff radius,  $r_{\text{cut}}$ , a buffer radius,  $r_{\text{buf}}$ , is used to keep track of neighbor molecules that might interact, not including in the neighbor list molecules that are further than  $r_{\text{buf}}$ . As default options, the  $r_{\text{buf}}$  is the half of the minimum length size of the box (`rbuf = Lmin/2`, default) and the  $r_{\text{cut}}$  is 92% of the  $r_{\text{buf}}$  (`rcut = 0.92rbuf`, default). This length of 8% for the  $r_{\text{buf}}$  was suggested in literature[3] as an optimum value for liquid systems, but it might be modified by the user to obtain a good compromise between the

---

\*henrique.cezar@usp.br

†canuto@if.usp.br

‡kaline@if.usp.br

number of steps needed between each neighbor list update and an effective reduction in the number of possible interacting molecules. The default update of the neighbor list is calculated based in simulations of liquid water at room conditions in different size boxes with default values of  $r_{\text{cut}}$  and  $r_{\text{buf}}$ , as `upbuf = int(( $r_{\text{buf}} - r_{\text{cut}}$ )/0.013)`. As examples, for simulations with  $N = 500$ , 1000 and 3000 water molecules, the `upbuf = 75`, 95 and 137, respectively.

Several default values are provided for the algorithmic options and parameters, and the automatic adjustment of parameters is done for some cases. The goal is to keep the simple input file for the user, but also allow the user to have control over the simulation. Even though the main focus is solute-solvent systems, the software tries to be general so different systems can be simulated.

## SI 1.2: Initialization and Metropolis MC

The algorithm implemented in the DICE starts by performing the initialization of the variables, reading the information from input files. At least three files are read (see Sec. SI 5 for examples): (i) a file with keywords information about the simulated ensemble, thermodynamic conditions, different types of molecules and their quantities, number of steps, algorithmic options and other information (Examples: `octane.ter`, `neopentane.txt`, `4ethylheptane.txt`, `dce.ter` and `subpc.ter` for thermalization stage and `octane.in`, `dce.in` and `subpc.in` for equilibrium stage); (ii) a file containing information of  $m$  different types of molecules that compose the system. For each molecule the information are: the quantity of atoms, the identification name (`namid`), the initial geometry (Cartesian coordinates) and the force field non-bonded parameters for each atom: charge  $q_i$  for the Coulomb potential and  $\epsilon_i$  and  $\sigma_i$  for the Lennard-Jones potential (Examples: `octane.txt`, `dce.txt` and `subpc.txt`); and (iii) a file containing the fragments composition and connections (`$atoms fragments` and `$fragment connection` blocks of data), topology and the force field bonded parameters (`$bond`, `$angle`, `$dihedral` and `$improper` blocks of data) for the flexible or semi-flexible molecules (Examples: `octane.dfr`, `dce.dfr` and `subpc.dfr`). Additionally, a file containing the initial configuration of the simulation may also be provided (`init = yesreadxyz`), otherwise, the initial configuration is generated randomly (`init = yes`).

After the initialization, the simulation starts. In the  $NVT$  ensemble, a new trial configuration, or one MC step, is always generated by selecting one molecule from the box (molecule  $A$ ), either randomly or with preferential sampling[4, 5] (`sampling = 2`). After selecting  $N$  molecules one MC cycle is completed. In each MC step, a rigid trial (translation and rotation at the center of mass) or a flexible trial (an internal deformation with the CBMC method) is performed with a specific ratio of flexible trial (`pcbmc = 0.5`, default). The flexible trial is performed only if the keyword `flex = nameid` exist in the input file `*.txt` and, in this case, a file `nameid.dfr` should also exist containing the fragments information. In the `*.dfr` file each fragment should be identified by its set of atoms and a label that defines its status: R for rigid, F for semi-flexible (rigid bonds only) and M for flexible. If a fragment is rigid, the fragment library for this specific fragment is not generated. If a fragment is semi-flexible or flexible, a fragment library will be generated in the pre-simulation stage where a simple MC

simulation of the isolated fragment is performed saving  $N_{sf}$  configurations (`nsf` = 10000, default) in a specific interval of steps (`sfint` = 500, default).

The rigid trial is composed by a random displacement of  $\delta x$ ,  $\delta y$  and  $\delta z$ , within a self-adjusted maximum value of  $\pm\delta r_{\max}$  performed in specific number of MC cycles (`nratio` = 50, default), and a random rotation around one of the Cartesian axis within a maximum values of  $\pm 15^\circ$ . In the  $NPT$  ensemble, additionally one trial that changes the volume of the simulation box and rescales the molecular center of mass is also performed considering an isotropic incremental factor  $\delta L$  within a self-adjusted maximum value of  $\pm\delta L_{\max}$  performed in specific number of MC cycles (`vratio` = 50, default). This volume trial is performed in a specific interval of MC cycles (`nstep` = 5, default). The self-adjusted maximum values,  $\delta r_{\max}$  and  $\delta L_{\max}$ , are used to keep the acceptance ratio of new configurations around 50% (`acceptance` = 0.5, default), but their are limited by an interval of 0.01 Å and 2.00 Å.

The potential energy of this new configuration is calculated and the acceptance of the trial move is tested. For the rigid trial the Eq. 6 or 7 is used for the Metropolis sampling or for the flexible trial the Eq. 19 or 24 is used for the CBMC sampling. If accepted, the new configuration replaces the old one, otherwise the old configuration accounts as a new one, and the values of energy, square energy and others properties of the new configuration are accumulated for later obtaining the thermodynamic properties. These steps are repeated until the total number of MC cycles required by the user is achieved. In Fig. S1 a flowchart shows the algorithm implemented in DICE.

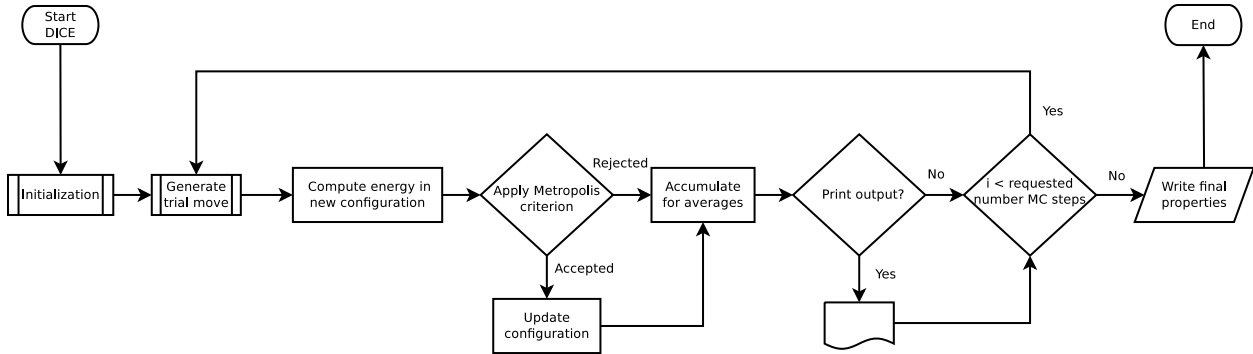


Figure S1: Flowchart of the Metropolis MC algorithm as implemented in DICE. More detail is given in the text.

The efficiency of the parallelization is measured in terms of the speedup  $S = \frac{t(1)}{t(n)}$ , with  $t(1)$  being the walltime for the run using a single thread and  $t(n)$  the walltime for the parallel run with  $n$  threads. We ran simulations of 4000 and 10 000 SPC/E water molecules in a box using the  $NPT$  ensemble for  $1.6 \times 10^7$  MC steps. The simulations were run in a node with two Xeon E5-2670 @ 2.60GHz and 64 GB of memory. Results are shown in Figure S2.

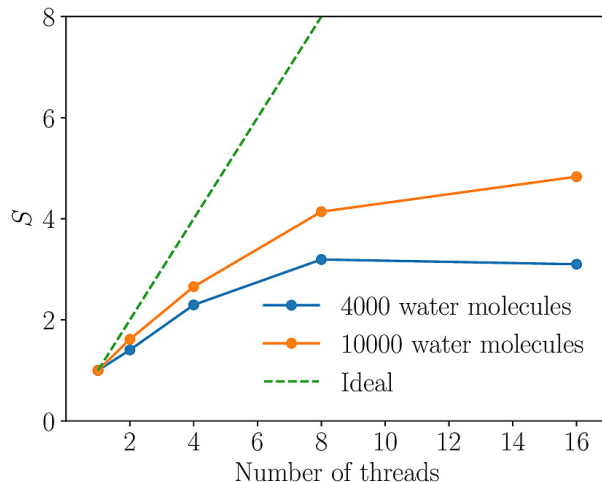


Figure S2: Speedup curve for a DICE parallel simulation in the  $NPT$  ensemble.

### SI 1.3: Generating the $\kappa_\phi$ trial insertion angles

In DICE, the complete CBMC move consists of 5 processes:

- a) breaking the flexible molecule with  $N_{frag}$  fragments in a random rotatable bond, with probability  $1/(N_{frag} - 1)$ ;
- b) selecting one of the two sides and deleting the fragments ( $N_{del}$ ) from this side, keeping the other side unchanged. The user can select between two possibilities for this choose:
  - (i) with 50% of chance for each side (`sweight = no`), or
  - (ii) with a weight that favors smaller parts to be sampled more often (`sweight = yes`, default), increasing the acceptance rates of the CBMC move. This choice is weighted by the number of atoms, and the side with less atoms is chosen more frequently with probability  $1 - (N_{smaller}/N)$ , where  $N_{smaller}$  is the number of atoms of the size with less atoms and  $N$  the total number of atoms of the molecule;
- c) selecting one configuration of each deleted fragment library with equal probability  $1/N_{sf}$ ;
- d) reconstructing the entire molecule connecting each fragment in the new configuration with a new dihedral angles selected with a probability proportional to the Boltzmann distribution in a small set of trial dihedral angles  $\kappa_\phi$ . Some option were implemented for this selection and will be discussed below; and
- e) calculating the probability of reconstructing the old conformation of the entire molecule with a similar procedure to obtain the acceptance criterion. In doing so, the old fragment configuration and the old dihedral angles should be selected.

The user can select between three different algorithms to select the trial insertion dihedral angles: (i) random  $\phi$  sampling; (ii) equidistant  $\phi$  sampling; and (iii) bias  $\phi$  sampling. The first two sampling are random (`biasphi = no`, default) and preliminary tests indicate that both algorithms give similar results. The random  $\phi$  sampling selects the  $\kappa_\phi$  angles (`ntrialphi = 16`, default) by drawing random values in the interval  $[0, 2\pi)$  (`equiphi = no`, default). The equidistant  $\phi$  sampling draws only one random angle in the same interval and then generates the other  $\kappa_\phi - 1$  trial angles by distributing the points uniformly in the circumference (`equiphi = yes`) with the same  $\Delta\phi$  value. Both algorithms make no assumption on the energy scales of the torsional and nonbonded energies.

When the minima of the torsional potential, have their positions close to the minima of the total potential energy, it is possible to improve the CBMC acceptance rate by introducing another bias. This additional bias is used while generating the  $\kappa_\phi$  trial insertion angles, favoring dihedral angles that results in lower torsional energies (`biasphi = yes`). We implemented this bias using the rejection method,[6, 7] accepting new angles with the probability  $\exp[-\beta u_{i\alpha}^{\text{dih}}(n)]$ , where  $u_{i\alpha}^{\text{dih}}(n)$  is the summation of all the torsional energies of the dihedral angles that unite the fragment  $i$  with the previous fragment. Introducing this bias removes the torsional energy from the  $P_{\text{soft}}$  probability of Eq. 14, leaving only the nonbonded energy to be used in the CBMC bias. Following the same steps, a Rosenbluth factor that does not depend on the torsional energy is obtained, and the same acceptance criterion of Eq. 19 can be used but with the different Rosenbluth factor definition, which contains only the nonbonded energy.

## SI 1.4: Force Field

In this version, DICE supports both OPLS[8] and AMBER[9] force fields to evaluate the energy. These force fields use simple harmonic functions to describe the bonded terms of the potential energy: bonds, angles and improper dihedral angles

$$\mathcal{U}_{\text{bond}} = \sum_i^{\text{bonds}} K_r^i (r_i - r_{\text{eq}})^2, \quad (\text{S1})$$

$$\mathcal{U}_{\text{angle}} = \sum_i^{\text{angles}} K_\theta^i (\theta_i - \theta_{\text{eq}})^2, \quad (\text{S2})$$

$$\mathcal{U}_{\text{improper}} = \sum_i^{\text{improper}} K_\phi^i (\phi_i - \phi_{\text{eq}})^2, \quad (\text{S3})$$

and also cosine functions for the improper dihedral angles

$$\mathcal{U}_{\text{improper}} = \sum_i^{\text{improper}} \frac{V_2^i}{2} [1 + \cos(2\phi_i - f_2^i)]. \quad (\text{S4})$$

For the proper dihedral (torsional) angles, two forms were implemented with a slightly different Fourier terms to describe the

$$\begin{aligned}
\mathcal{U}_{\text{torsion}}^{\text{OPLS}} = & \sum_i^{\text{dihedral}} \frac{V_1^i}{2} [1 + \cos(\phi_i + f_1^i)] \\
& + \frac{V_2^i}{2} [1 - \cos(2\phi_i + f_2^i)] \\
& + \frac{V_3^i}{2} [1 + \cos(3\phi_i + f_3^i)] \\
& + \frac{V_4^i}{2} [1 - \cos(4\phi_i + f_4^i)],
\end{aligned} \tag{S5}$$

and

$$\begin{aligned}
\mathcal{U}_{\text{torsion}}^{\text{AMBER}} = & \sum_i^{\text{dihedral}} \frac{V_1^i}{2} [1 + \cos(\phi_i - f_1^i)] \\
& + \frac{V_2^i}{2} [1 + \cos(2\phi_i - f_2^i)] \\
& + \frac{V_3^i}{2} [1 + \cos(3\phi_i - f_3^i)] \\
& + \frac{V_4^i}{2} [1 + \cos(4\phi_i - f_4^i)].
\end{aligned} \tag{S6}$$

The Lennard-Jones (LJ) and Coulomb (Q) potentials are used to describe the atomic pairwise non-bonded interactions

$$\mathcal{U}_{ij} = \mathcal{U}_{ij}^{\text{LJ}} + \mathcal{U}_{ij}^{\text{Q}} = f_{ij}^{\text{LJ}} 4\epsilon_{ij} \left[ \left( \frac{\sigma_{ij}}{r_{ij}} \right)^{12} - \left( \frac{\sigma_{ij}}{r_{ij}} \right)^6 \right] + f_{ij}^{\text{Q}} \frac{q_i q_j e^2}{(4\pi\epsilon_0)r_{ij}} \tag{S7}$$

where  $e^2/(4\pi\epsilon_0) = 331.9684 \text{ \AA kcal/mol}$ ,  $\epsilon_{ij} = \sqrt{\epsilon_i \epsilon_j}$ ,  $\sigma_{ij} = \sqrt{\sigma_i \sigma_j}$  or  $\sigma_{ij} = (\sigma_i + \sigma_j)/2$  depending on the input option and  $\epsilon_i$ ,  $\sigma_i$  and  $q_i$  are the atomic parameters. For the intermolecular interactions, i.e.  $i$  and  $j$  belong to different molecules,  $f_{ij}^{\text{LJ}} = f_{ij}^{\text{Q}} = 1$ . For the intramolecular interactions, i.e.  $i$  and  $j$  belong to the same molecule, the  $f_{ij}$  assumes different values depending on the force field and also on the number of bonds that separate the atoms within the molecule. Atoms separated by one bond, 1-2, and two bonds, 1-3, interact only through the bonded terms, then  $f_{ij}^{\text{LJ}} = f_{ij}^{\text{Q}} = 0$ . The atoms separated by three bond, 1-4, have a scaling factor in the non-bonded interaction:  $f_{ij}^{\text{Q}} = f_{ij}^{\text{LJ}} = 0.5$  for the OPLS force field (`fudge1j = 0.5` and `fudge1b = 0.5`) and  $f_{ij}^{\text{LJ}} = 0.5$  and  $f_{ij}^{\text{Q}} = 1/1.2$  for the AMBER (`fudge1j = 0.5` and `fudge1b = 0.8333`). For atoms separated by four bonds or more, the interactions are calculated considering only non-bonded interaction without any scaling factor, then  $f_{ij}^{\text{LJ}} = f_{ij}^{\text{Q}} = 1$ .

Therefore, the total potential energy of a molecule  $A$  is calculated considering all explicit interactions (intra and intermolecular) within the cutoff radius  $r_{\text{cut}}$  and the long range

correction (LRC)

$$\mathcal{U}^A = \mathcal{U}_{\text{intra}}^A + \mathcal{U}_{\text{inter}}^A + \mathcal{U}_{\text{LJ-LRC}}^A + \mathcal{U}_{\text{Q-LRC}}^A \quad (\text{S8})$$

where

$$\mathcal{U}_{\text{intra}}^A = \mathcal{U}_{\text{bond}} + \mathcal{U}_{\text{angle}} + \mathcal{U}_{\text{torsion}} + \mathcal{U}_{\text{improper}} + \sum_{\substack{i=1 \\ i \in A}}^{N_A-1} \sum_{\substack{j=i+1 \\ j \in A}}^{N_A} \mathcal{U}_{ij} \quad (\text{S9})$$

and

$$\mathcal{U}_{\text{inter}}^A = \sum_B \sum_{\substack{i=1 \\ i \in A}}^{N_A} \sum_{\substack{j=1 \\ j \in B}}^{N_B} \mathcal{U}_{ij}, \quad (\text{S10})$$

which  $B$  are the other molecules inside  $r_{\text{cut}}$  and  $R_{AB}$  are the center of mass distance between  $A$  and  $B$ .

The two LRC terms are approximations to calculate the energy contribution given by molecules with  $r_{\text{cut}} < R_{AB} \leq \infty$ . For the Lennard-Jones potential, an uniform distribution of molecules is assumed beyond  $r_{\text{cut}}$  to infinity, i.e.  $g(r_{ij}) \approx 1$ , then

$$\mathcal{U}_{\text{LJ-LRC}}^A = 2\pi N \rho \sum_B \sum_{\substack{i=1 \\ i \in A}}^{N_A} \sum_{\substack{j=1 \\ j \in B}}^{N_B} \frac{4\epsilon_{ij}\sigma_{ij}^3}{9} \left[ \left( \frac{\sigma_{ij}}{r_{ij}} \right)^9 - 3 \left( \frac{\sigma_{ij}}{r_{ij}} \right)^3 \right] \quad (\text{S11})$$

which  $B$  are the molecule types that compose the system.

For the Coulomb potential, an dielectric continuum larger than 1.0 is assumed beyond  $r_{\text{cut}}$  to infinity, generating a reaction field (`dielectric` = 1.0, default, does not calculate the LRC term for the Coulomb potential). Therefore, it is necessary to define the keyword `dielectric` with a value larger than 1.0 to take this term into account. We implemented two models for the reaction field: (i) the model discussed by Barker and Watts[10] with the equation well presented in Ref. [11] (`electrostatics` = `reaction-field`) and (ii) the model discussed in Allen and Tildesley with the additional Born term[3] (`electrostatics` = `reaction-field-born`, default).

The first model is similar to the model implemented in other software like GROMACS

$$\mathcal{U}_{\text{Q-LRC}}^A = \sum_B \sum_{\substack{i=1 \\ i \in A}}^{N_A} \sum_{\substack{j=i \\ j \in B}}^{N_B} q_i q_j \left( \frac{\epsilon_{\text{RF}} - 1}{2\epsilon_{\text{RF}} + 1} \frac{r_{ij}^2}{r_{\text{cut}}^3} + \mathcal{C} \right) \quad (\text{S12})$$

where  $\epsilon_{\text{RF}}$  is the dielectric constant of the continuum and the constant  $\mathcal{C}$  is

$$\mathcal{C} = -\frac{3\epsilon_{\text{RF}}}{2\epsilon_{\text{RF}} + 1} \frac{1}{r_{\text{cut}}}. \quad (\text{S13})$$

When the conformational change of molecule  $A$  is performed in the CBMC step, we also take into account the self energy correction of the dielectric continuum

$$\mathcal{U}_{\text{self}}^A = \sum_{\substack{i=1 \\ i \in A}}^{N_A-1} \sum_{\substack{j=i+1 \\ j \in A}}^{N_A} q_i q_j \left( \frac{\epsilon_{\text{RF}} - 1}{2\epsilon_{\text{RF}} + 1} \frac{r_{ij}^2}{r_{\text{cut}}^3} + \mathcal{C} \right) \quad (\text{S14})$$

This contribution is constant if the molecule is rigid and, therefore, cancels in the Metropolis acceptance criterion that considers the energy variation of the molecule  $A$  in the old and new configurations,  $\Delta\mathcal{U}^A$ .

In the second model, the potential energy long range correction due to the electrostatic field on molecule  $A$ , considering the Born correction, is given by

$$\mathcal{U}_{\text{Q-LRC-RFB}}^A = \mathcal{U}_{\text{Q-LRC}}^A + \mathcal{U}_{\text{Born}}^A, \quad (\text{S15})$$

where

$$\mathcal{C} = \mathcal{C}_{\text{RFB}} = -\frac{1}{r_{\text{cut}}} \left( 1 + \frac{\epsilon_{\text{RF}} - 1}{2\epsilon_{\text{RF}} + 1} - \frac{\epsilon_{\text{RF}} - 1}{\epsilon_{\text{RF}}} \right) \quad (\text{S16})$$

and

$$\mathcal{U}_{\text{Born}}^A = - \sum_{B}^{R_{AB} \leq r_{\text{cut}}} \left( \frac{\epsilon_{\text{RF}} - 1}{\epsilon_{\text{RF}}} \right) \frac{1}{r_{\text{cut}}} Q_A Q_B, \quad (\text{S17})$$

with  $Q_A$  and  $Q_B$  being the total charges of molecules  $A$  and  $B$ , respectively. The self polarization term is also considered with  $\mathcal{C}_{\text{RFB}}$  when the CBMC moves are performed.

## SI 2: n-octane

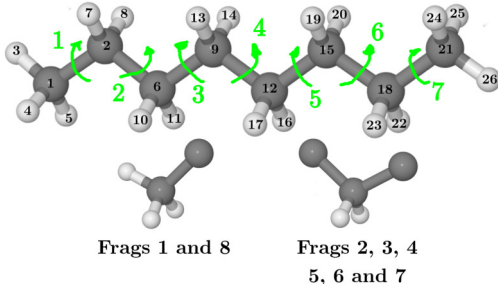


Figure S3: n-octane molecule with the atomic labels and its fragments. The green arrows and numbers indicate the rotatable bonds and its indexes.

### SI 2.1: Acceptance rates for different $\kappa_\phi$ for n-octane in gas phase

To show the dependence of the acceptance rates and walltime with the number of trial insertion angles  $\kappa_\phi$  we have performed simulations of n-octane in gas phase considering  $\kappa_\phi = 8, 12, 16, 18, 24, 32$  and  $64$  and all other parameters as detailed in the main text. The simulations were run for  $10^6$  CBMC steps under the same conditions in a desktop PC equipped with an Intel Core i7 3930K running at 3.2 GHz and 64 GB of RAM running at 1333 MHz. The DICE OpenMP parallelization with 6 threads was employed. After the selection of the rotatable bond in each CBMC step, the side was selected considering the number of atoms attached to each extremity, favoring the side with less atoms (**sweight**



= yes). This option increases the acceptance rates, as the regrowing a smaller side of the molecule with few fragments usually yields higher acceptance rates than regrowing the large side with several fragments.

In Table S1 we show the overall and partial acceptance rates (for each rotatable bond), as well as the average walltime, or the elapsed real time, for three runs. The walltime does not consider the time needed to generate the fragment library, which takes approximately  $(41.2 \pm 0.3)$ s. Each rotatable bond was selected an equivalent number of times during the simulation, and the acceptance rates for each bond take into account the probability of accepting the CBMC move independent on which side of the rotatable bond was deleted. Therefore, the acceptance rate is an average of two rates that may be different depending on how many fragments need to be reinserted on that side. The acceptance rates vary less than 2% considering runs with different seeds.

Table S1: Acceptance rate (%) for a simulations of n-octane with different number of trial insertion angles  $\kappa_\phi$ . The bonds are labeled according to Figure S3. The walltime was obtained as an average of 3 runs. The data shown in this table is an output of DICE in the `outname.acb` file.

$\kappa_\phi =$	$\kappa_\phi$						
	8	12	16	18	24	32	64
bond 1	65.9	68.7	71.8	72.7	73.9	75.4	77.6
bond 2	33.6	38.1	43.1	44.4	47.5	50.8	56.2
bond 3	18.8	22.9	27.9	29.4	33.0	37.3	44.2
bond 4	14.8	18.6	23.4	25.2	29.1	33.8	41.1
bond 5	19.3	23.3	27.9	29.6	33.7	38.0	44.1
bond 6	33.4	38.2	42.3	43.3	46.9	50.0	55.2
bond 7	65.7	69.5	71.6	72.3	73.9	75.4	77.4
overall	35.9	39.9	44.0	45.3	48.3	51.6	56.6
Walltime (s)	86.3	89.4	103.3	104.9	120.8	148.3	222.0

As we see on Table S1, by increasing the number of trial insertion angles, the acceptance rates increase, but so does the walltime. For a linear chain like n-octane, the lower acceptance rates are found in the middle of the chain, like bonds 3, 4 and 5. Indeed, the lowest acceptance rate is found for the rotatable bond 4, which has the similar acceptance probabilities for both sides of the bond. Increasing the number of trial insertion angles from 8 to 64, an increase of almost 27% is observed for the acceptance rate of the rotatable bond 4. However, while the walltime increase of 2.5 times is not relevant for the gas phase simulation, it becomes important, and also more dramatic, when the solvent is considered, since for each trial insertion position the interaction with the solvent is computed. Therefore, the user should find an equilibrium between acceptance rate and computational time.

The rotatable bonds close to the extremities, like bonds 1 and 7, have a high acceptance rate independent on the number of trial insertion angles. This happens because when the

side to be regrown is the side relative to the  $C_2H_3$  fragment (methyl group, fragments 1 and 8), just one fragment needs to be inserted, and the acceptance rates for this insertion are as high as 77% for  $\kappa_\phi = 8$  and 87% for  $\kappa_\phi = 64$ . Reinserting the other side of bonds 1 and 7 (which is basically regrowing the whole molecule), however, is more difficult, resulting in acceptance rates of 4% and 24% for  $\kappa_\phi = 8$  and 64, respectively. The number shown in Table S1 is the weighted average, considering that the whole molecule is regrown only 15% of the times that the rotatable bonds 1 and 7 are selected.

## SI 2.2: Equilibrium constant of n-octane and rotational potential

Assuming just three possible configurations accessible to the system: *trans* ( $T$ ), *gauche*(+) ( $G+$ ) e *gauche*(-) ( $G-$ ), we have that the concentrations must sum to 100%

$$[T] + [G+] + [G-] = 1. \quad (S18)$$

Considering the symmetry of the potential among the *gauche*(+) and *gauche*(-) conformations, we should have equal concentrations of these two conformers:

$$[G+] = [G-]. \quad (S19)$$

The equilibrium constant  $K$  giving the conformational changes between the *trans* and *gauche*(+) conformation is then

$$K = \frac{[G+]}{[T]} = \frac{[G+]}{1 - 2[G+]}, \quad (S20)$$

from which we obtain the population of *gauche*+ conformations

$$[G+] = \frac{K}{2K + 1}. \quad (S21)$$

Since the equilibrium constant is related to the Gibbs free energy with the expression

$$K = e^{\frac{-\Delta G}{kT}}, \quad (S22)$$

with  $k$  being the Boltzmann constant,  $T$  is the temperature and  $\Delta G$  is the free energy difference between the *trans* and *gauche*(+) conformations. Additionally, when an isolated molecule is studied the approximation of  $\Delta G \approx \Delta E - T\Delta S$  can be used considering a negligible enthalpic contributions ( $P\Delta V \approx 0$ ). The energy differences,  $\Delta E$  are in general obtained by quantum mechanics (QM) calculations of both conformations at the optimized geometry. The vibrational contribution of entropic term,  $T\Delta S$  can also be calculated by QM calculations. Therefore, the classical force field can be built considering the energetic and entropic contributions,  $\Delta E_{FF} = \Delta E_{QM} + T\Delta S_{QM}$  or only the energetic contribution assuming a negligible entropic contribution,  $\Delta E_{FF} = \Delta E_{QM}$ . Then, using the approximation of  $\Delta G \approx \Delta E_{FF}$ , we can finally estimate the *gauche*(+) population, determining the *gauche*(-) and *trans* populations too.

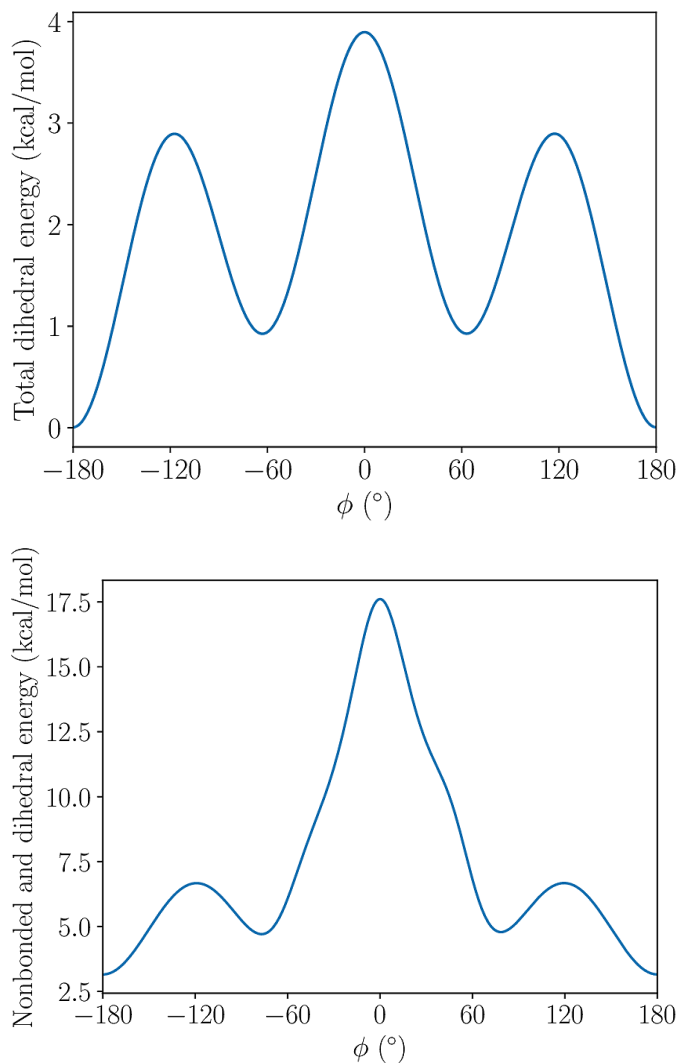


Figure S4: The energy profile of the OPLS-AA force field for the n-octane rotating around the C9-C12 bond with two rigid parts: (top) only the torsional angle and (bottom) the total energy including the bonded and non-bonded terms of the potential. In the torsional energy a global minimum is observed in  $\pm 180^\circ$ , *trans* form, and another two minima is observed in  $\pm 60^\circ$ , *gauche*( $\pm$ ) forms, with  $\Delta E(\text{trans} \rightarrow \text{gauche}) = 0.9$  kcal/mol and barriers of  $\Delta E^*(\text{trans} \rightarrow \text{gauche}) = 2.9$  kcal/mol and  $\Delta E^*(\text{gauche} \rightarrow \text{gauche}) = 3.9$  kcal/mol. Considering only this torsional energy, the  $\Delta E(\text{trans} \rightarrow \text{gauche}) = 0.9$  kcal/mol gives a *trans:gauche* population ratio of 70:30. In the total energy the global minimum still in *trans* form and the other two minima in *gauche*( $\pm$ ) forms shifted to around  $\pm 75^\circ$  with  $\Delta E(\text{trans} \rightarrow \text{gauche}) = 1.6$  kcal/mol and barriers of  $\Delta E^*(\text{trans} \rightarrow \text{gauche}) = 3.5$  kcal/mol and  $\Delta E^*(\text{gauche} \rightarrow \text{gauche}) = 12.8$  kcal/mol. Considering the total rotational energy, the  $\Delta E(\text{trans} \rightarrow \text{gauche}) = 1.6$  kcal/mol gives a *trans:gauche* population ratio of 88:12. We considered these populations as theoretical ideal values because they were obtained with rigid n-octane rotation not including the angles relaxation that were considered in our simulations.

### SI 2.3: Simulations analysis

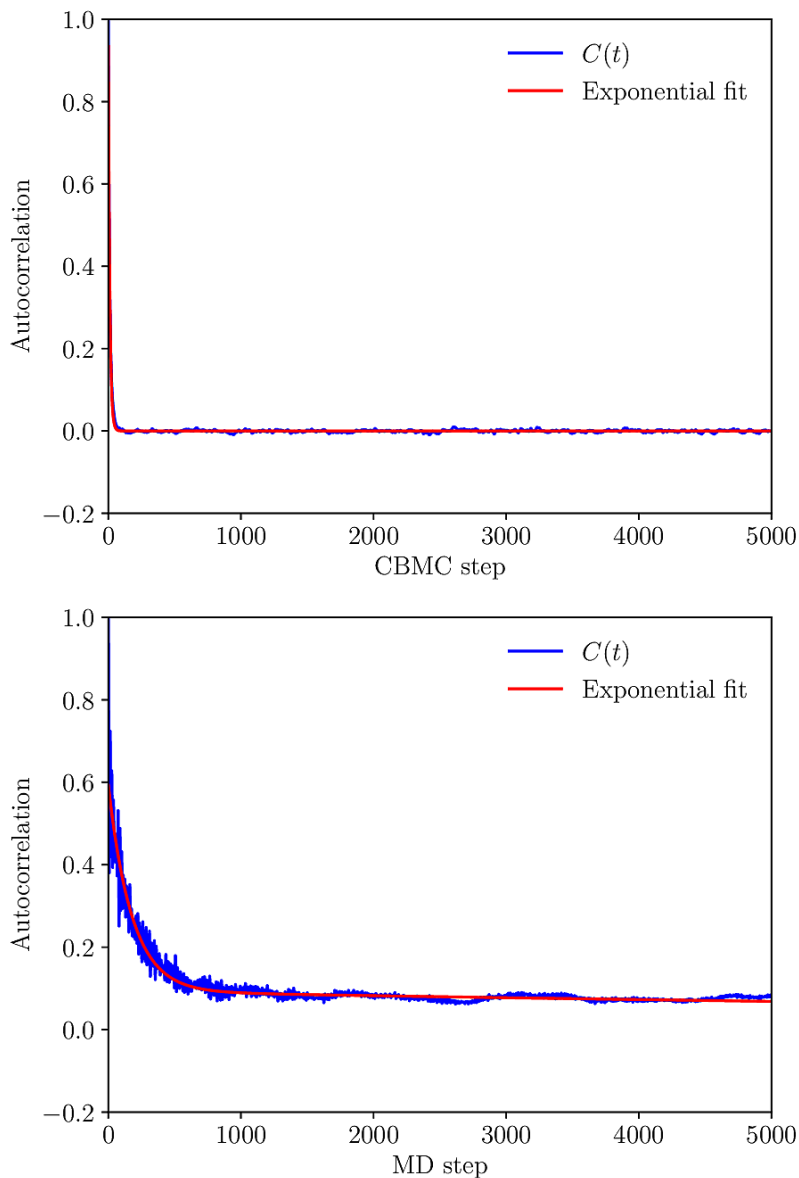


Figure S5: The autocorrelation function for the energy of the isolated n-octane simulations with CBMC (top) and MD (bottom). The fitted functions were two exponential decay,  $C(t) = w_1 e^{-t/\tau_1} + w_2 e^{-t/\tau_2}$  where  $w_1 = 9.33 \times 10^{-1}$ ,  $\tau_1 = 1.11 \times 10^1$ ,  $w_2 = 2.50 \times 10^{-4}$  and  $\tau_2 = 9.44 \times 10^4$  (top) and  $w_1 = 4.99 \times 10^{-1}$ ,  $\tau_1 = 1.78 \times 10^2$ ,  $w_2 = 9.28 \times 10^{-2}$  and  $\tau_2 = 1.64 \times 10^4$  (bottom). The statistical correlation interval (or time) was obtained as  $s = 2\tau$ , with  $\tau = w_1\tau_1 + w_2\tau_2$  by the integration of  $C(t)$ . Then,  $s_{\text{CBMC}} = 68$  and  $s_{\text{MD}} = 3225$ . Therefore, the CBMC method generate statistically uncorrelated configurations faster than MD method, in this case around 50 times.

Table S2: Average and standard deviation of the angles from the sampled n-octane configurations in CBMC and MD simulations of the isolated molecule and in chloroform solution. All values are in  $^{\circ}$  and they show a very good agreement between both simulations, as expected.

	Isolated		In chloroform	
	CBMC	MD	CBMC	MD
H-CH3-CH2	111.6 $\pm$ 4.4	111.4 $\pm$ 4.5	111.2 $\pm$ 4.6	111.4 $\pm$ 4.6
H-CH3-H	107.6 $\pm$ 4.8	107.6 $\pm$ 4.9	107.6 $\pm$ 4.7	107.6 $\pm$ 4.9
CH3-CH2-CH2	113.1 $\pm$ 3.4	112.7 $\pm$ 3.5	113.1 $\pm$ 3.4	112.7 $\pm$ 3.4
H-CH2-CH2	110.2 $\pm$ 4.3	110.0 $\pm$ 4.4	109.8 $\pm$ 4.4	110.0 $\pm$ 4.5
H-CH2-H	106.2 $\pm$ 4.7	106.5 $\pm$ 4.8	106.3 $\pm$ 4.8	106.5 $\pm$ 4.8
CH2-CH2-CH2	113.1 $\pm$ 3.4	112.8 $\pm$ 3.5	113.0 $\pm$ 3.4	112.8 $\pm$ 3.5

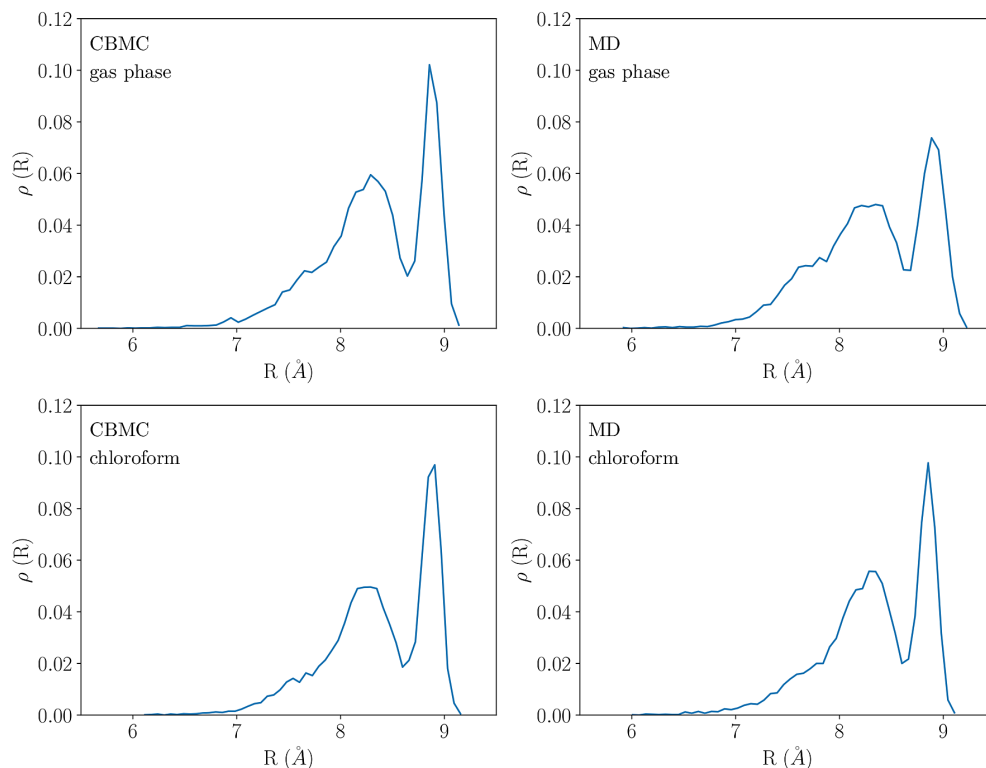


Figure S6: Calculated distribution of end-to-end lengths  $R$  of sampled n-octane configurations in CBMC and MD simulations of the isolated molecule (gas phase) and in chloroform solution. The well defined peak at larger lengths (between 8.7 Å and 9.1 Å) describes the all-trans conformation and the broad and asymmetrical peak at low lengths (between 6.5 Å and 8.7 Å) describes the other conformations mixing the *trans* and *gauche* forms of the five dihedral angles of n-octane.

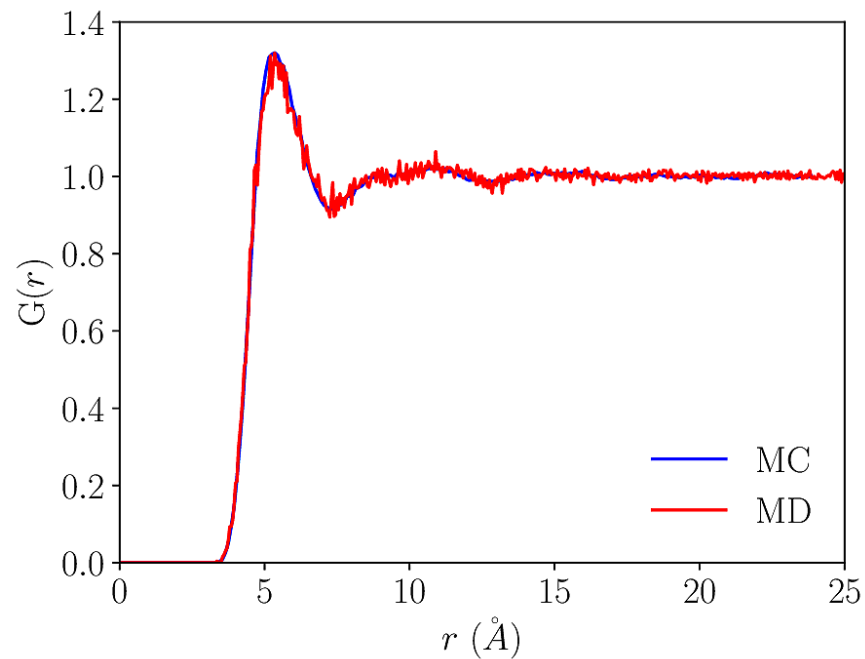


Figure S7: Radial distribution function  $G(r)$  between the center of mass of octane and the center of mass of the chloroform molecules, calculated using the CBMC simulation (blue) with  $10^5$  configurations and MD simulation (red) with  $10^4$  configurations. As one can see, the agreement between the curves show that the solvation shells are the same, independent of the method used for the simulation.

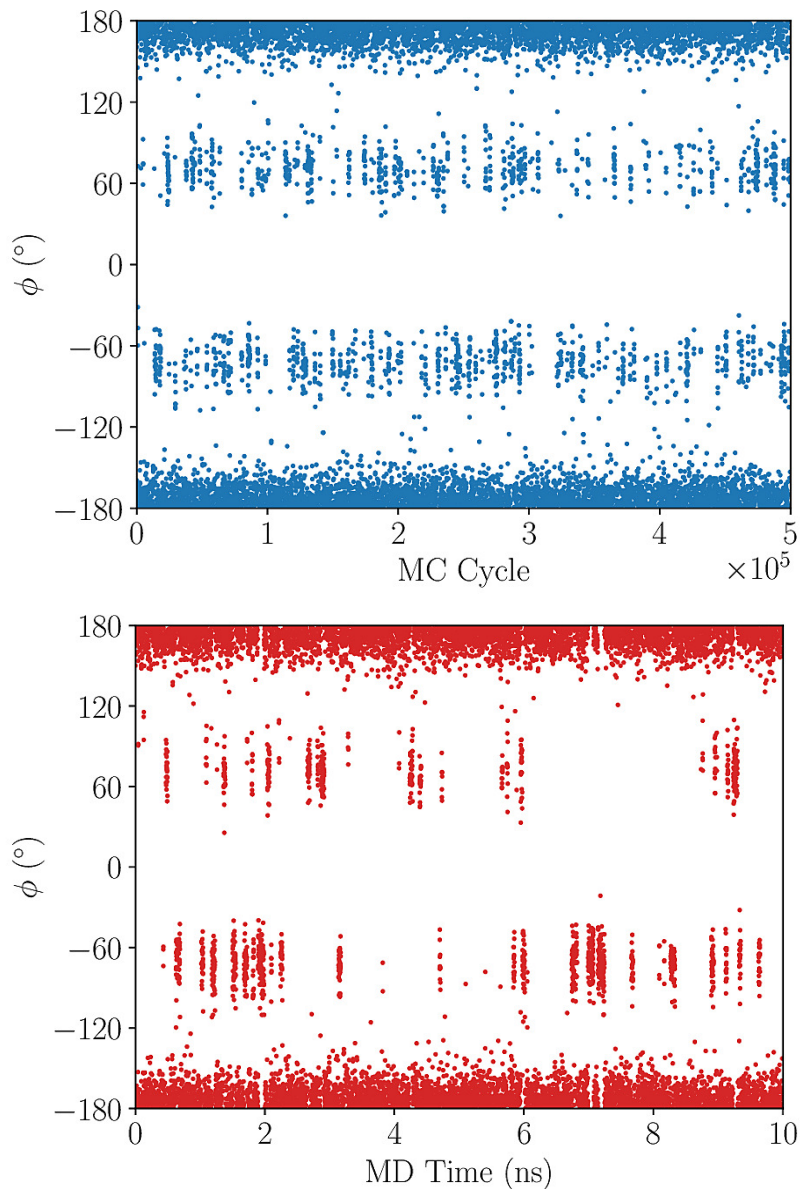


Figure S8: Evolution of the dihedral angle C6-C9-C12-C15 of n-octane in chloroform with simulation steps. Similar to the isolated molecule, the *gauche*(-), *gauche*(+) and *trans* forms can be easily identified and in the CBMC simulation the frequency of barrier crossing is still larger than that obtained in the MD simulation. The vertical strips in the MD distribution are more defined than in CBMC distribution and it describes the time interval where the conformation is trapped in the energy minimum. Additionally, in the MD distribution an asymmetry shows up between the *gauche*(-) and *gauche*(+) forms, which the *gauche*(-) has a larger occurrence than *gauche*(+) form, indicating the need of a larger MD simulation to improve the statistics of the frequency of barrier crossing.

### SI 3: DCE

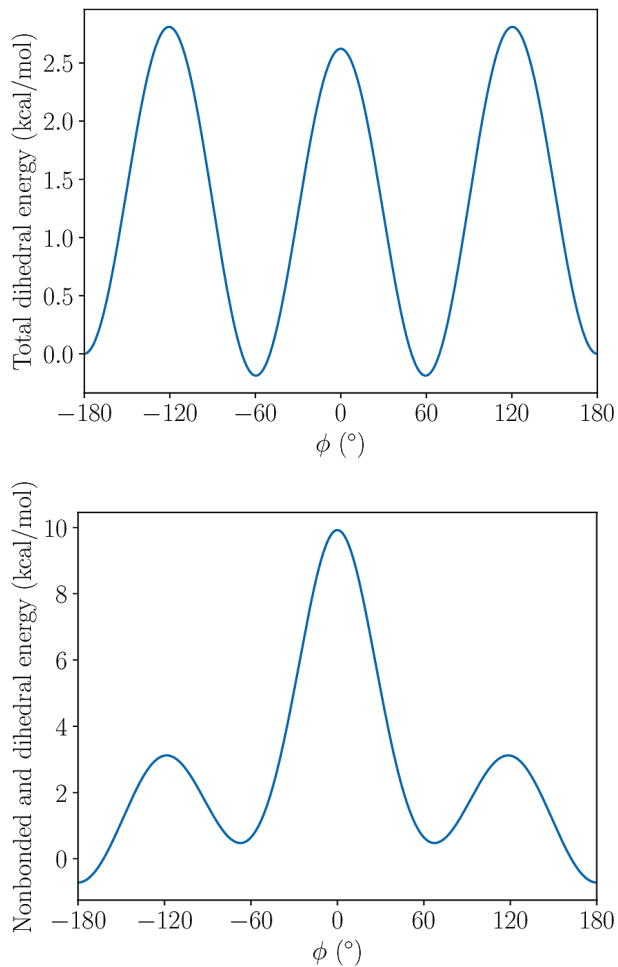


Figure S9: The energy profile of the OPLS-AA force field for the DCE rotating around the C-C bond with two rigid parts: (top) only the torsional angle and (bottom) the total energy including the bonded and non-bonded terms of the potential. In the torsional energy a global minima are observed around  $\pm 60^\circ$ , *gauche* form, and another minimum is observed in  $\pm 180^\circ$ , *trans* forms, with  $\Delta E(\text{trans} \rightarrow \text{gauche}) = -0.2 \text{ kcal/mol}$  and barriers of  $\Delta E^*(\text{trans} \rightarrow \text{gauche}) = 2.8 \text{ kcal/mol}$  and  $\Delta E^*(\text{gauche} \rightarrow \text{gauche}) = 2.6 \text{ kcal/mol}$ . Considering only this torsional energy, the  $\Delta E(\text{trans} \rightarrow \text{gauche}) = -0.2 \text{ kcal/mol}$  gives a *trans:gauche* population ratio of 26:73. In the total energy the global minimum now in *trans* form and the other two minima in *gauche*( $\pm$ ) forms shifted to around  $\pm 70^\circ$  with  $\Delta E(\text{trans} \rightarrow \text{gauche}) = 1.2 \text{ kcal/mol}$  and barriers of  $\Delta E^*(\text{trans} \rightarrow \text{gauche}) = 3.8 \text{ kcal/mol}$  and  $\Delta E^*(\text{gauche} \rightarrow \text{gauche}) = 9.4 \text{ kcal/mol}$ . Considering the total rotational energy, the  $\Delta E(\text{trans} \rightarrow \text{gauche}) = 1.2 \text{ kcal/mol}$  gives a *trans:gauche* population ratio of 80:20. We considered these populations as theoretical ideal values because they were obtained with rigid DCE rotation not including the bonds and angles relaxation that were considered in our simulations.



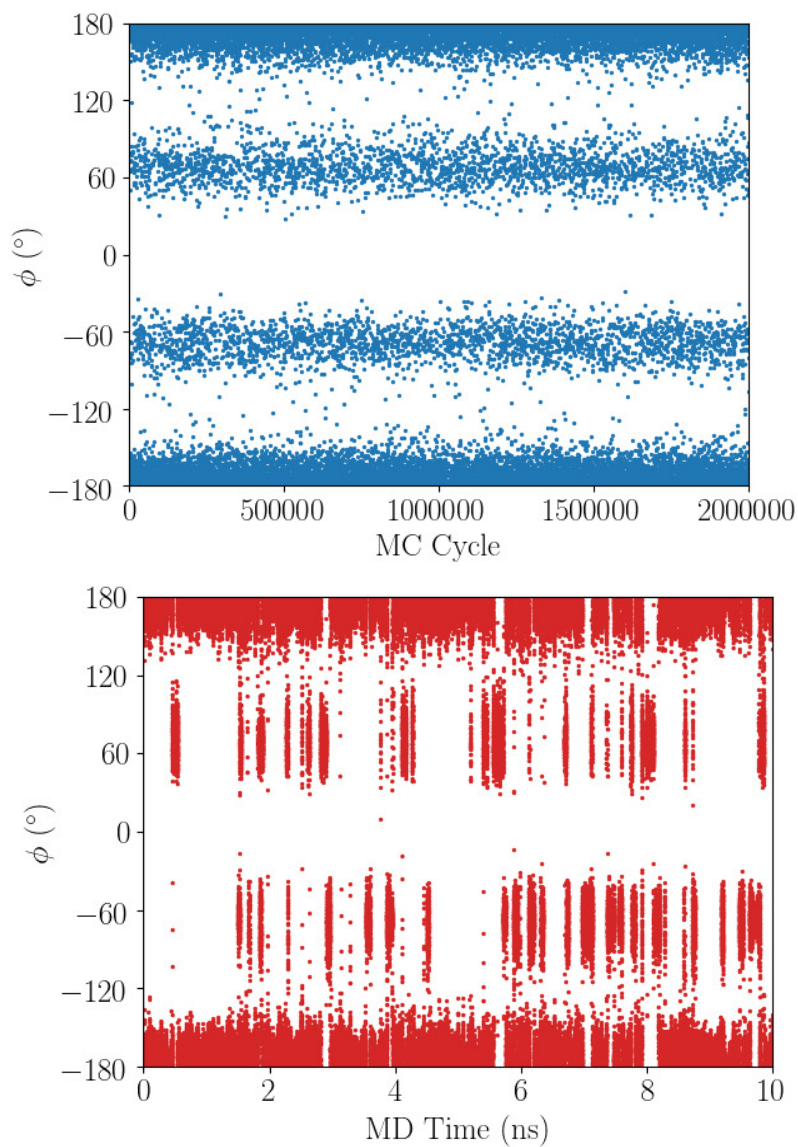


Figure S10: Evolution of the dihedral angle Cl-C-C-Cl of isolated DCE with simulation steps. The *gauche*(-), *gauche*(+) and *trans* forms can be easily identified with a larger density at the *trans* form. In the CBMC simulation the distribution is more uniform showing a larger frequency of barrier crossing than that obtained in the MD simulation. The vertical strips in the MD distribution are well defined and show the time interval where the conformation is trapped in the energy minimum.

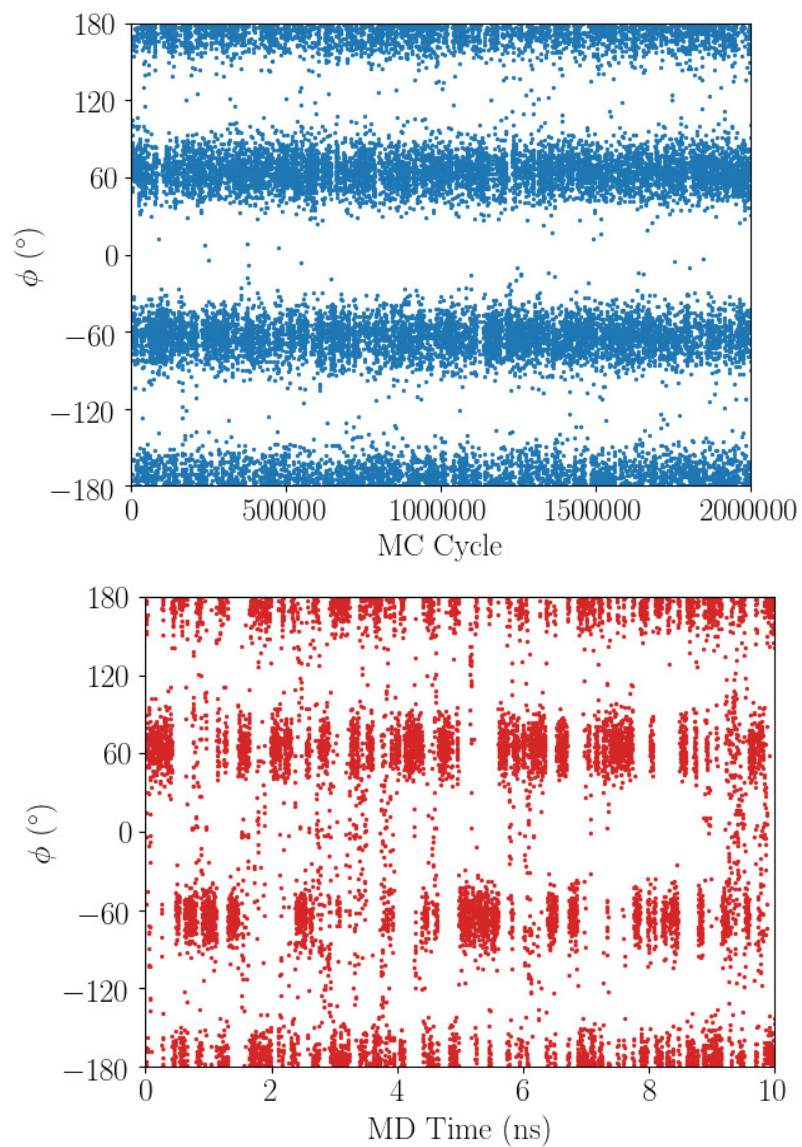


Figure S11: Evolution of the dihedral angle Cl-C-C-Cl of liquid DCE with simulation steps. Comparatively with the isolated DCE (see Fig. S10), it can be notice a increasing in the *gauche* form.

## SI 4: Data from the SubPC simulations

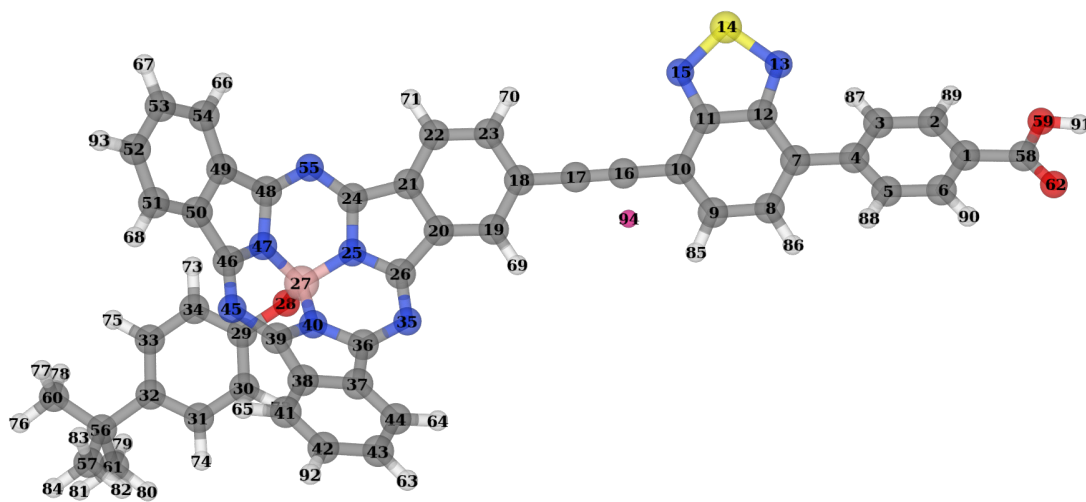


Figure S12: SubPC molecule with numeric labels for the atoms.

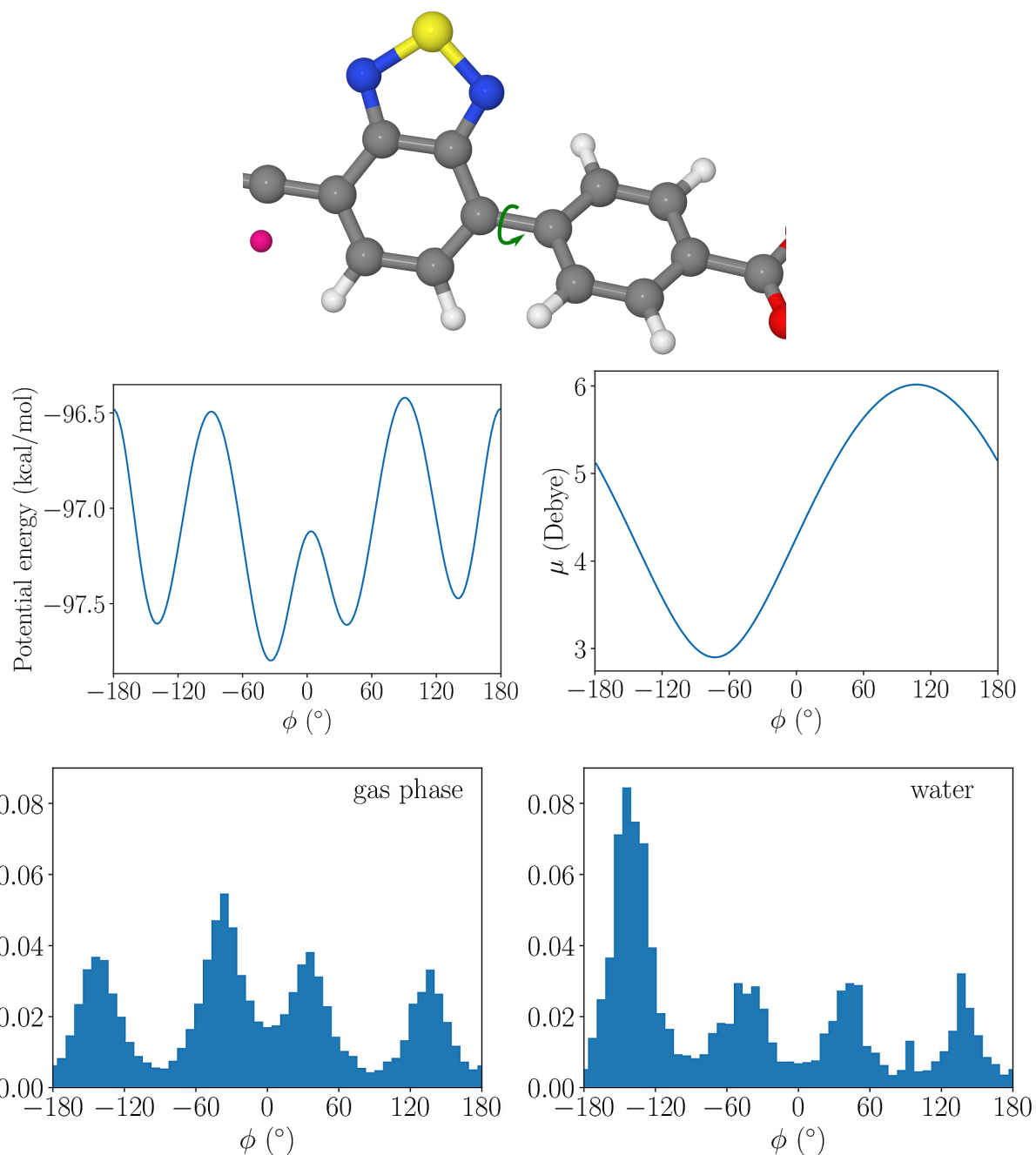


Figure S13: Top: Illustration the dihedral rotation  $D1$  between fragments 1 and 2; Middle left: The total energy profile involved in this rotation (C5-C4-C7-C8) for the isolated SubPC; Middle Right: Dipole moment  $\mu$  as a function of the rotation; Bottom left: Dihedral distribution obtained with the CBMC simulation of the isolated SubPC (gas phase); and Bottom right: Distribution obtained with the CBMC simulation of SubPC in water.

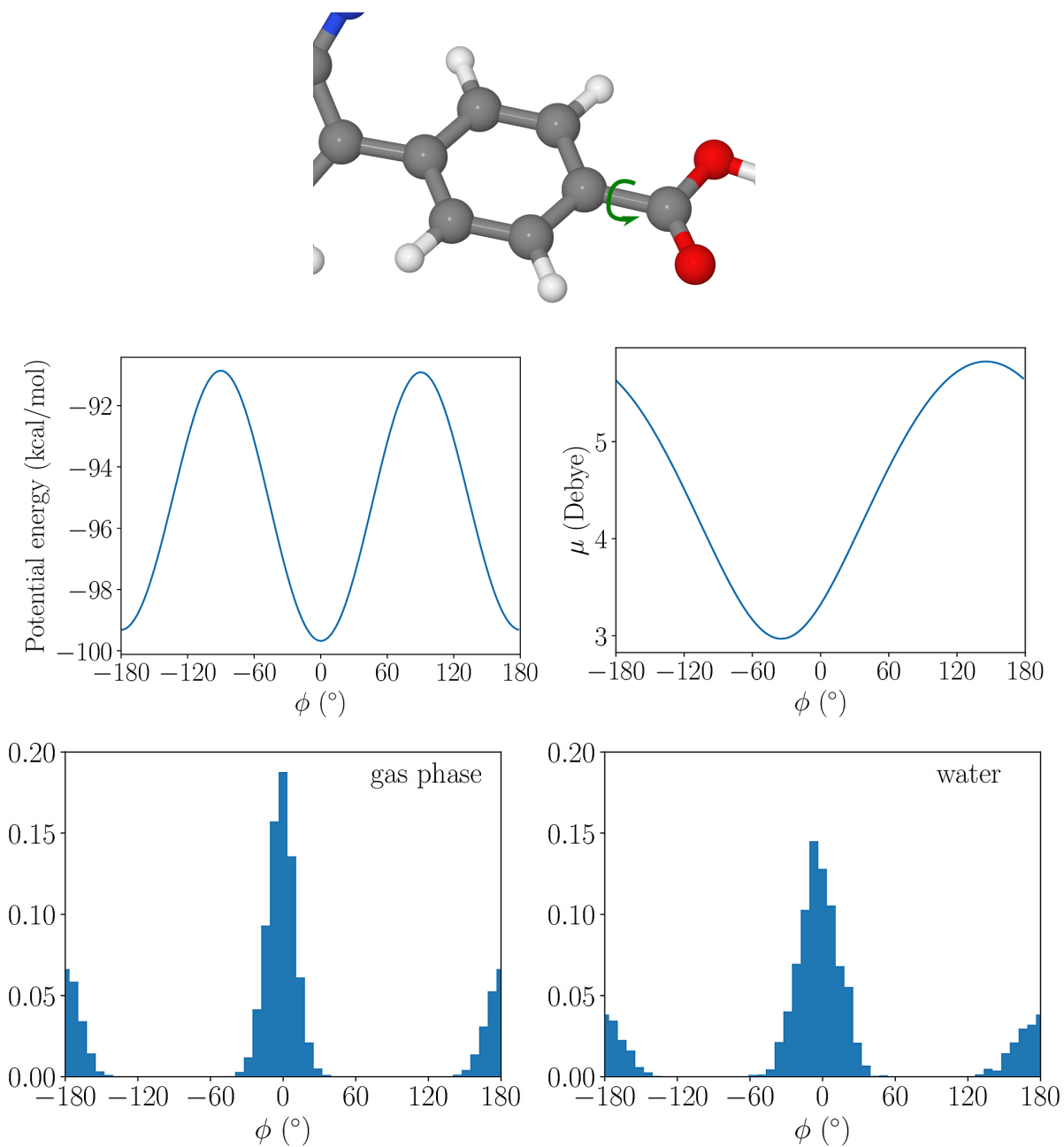


Figure S14: Top: Illustration the dihedral rotation  $D2$  between fragments 1 and 8; Middle left: The total energy profile involved in this rotation (C6-C1-C58-O62) for the isolated SubPC; Middle Right: Dipole moment  $\mu$  as a function of the rotation; Bottom left: Dihedral distribution obtained with the CBMC simulation of the isolated SubPC (gas phase); and Bottom right: Distribution obtained with the CBMC simulation of SubPC in water.

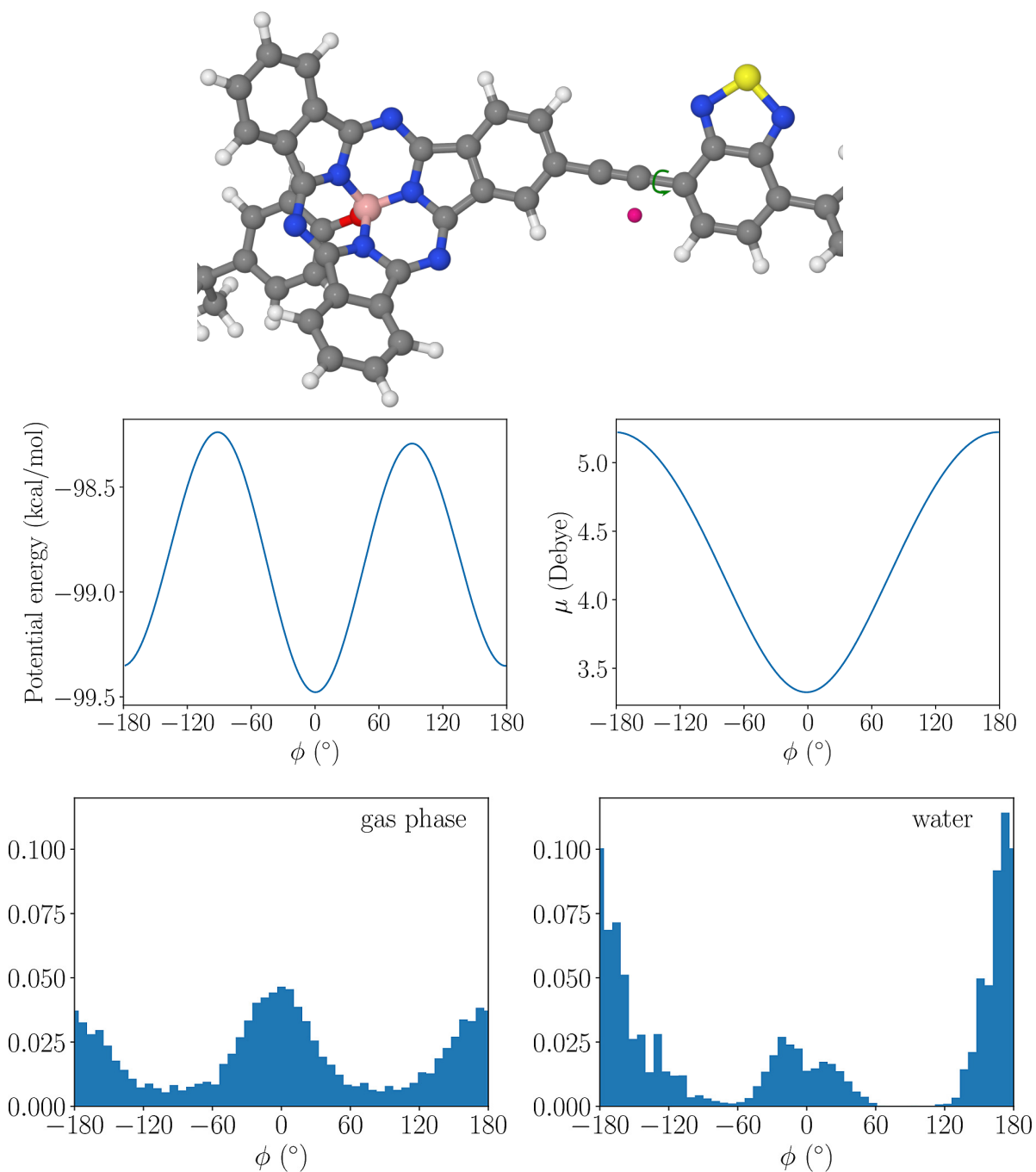


Figure S15: Top: Illustration the dihedral rotation  $D3$  between fragments 2 and 3; Middle left: The total energy profile involved in this rotation (C9-C10-C16-Xx94) for the isolated SubPC; Middle Right: Dipole moment  $\mu$  as a function of the rotation; Bottom left: Dihedral distribution obtained with the CBMC simulation of the isolated SubPC (gas phase); and Bottom right: Distribution obtained with the CBMC simulation of SubPC in water.

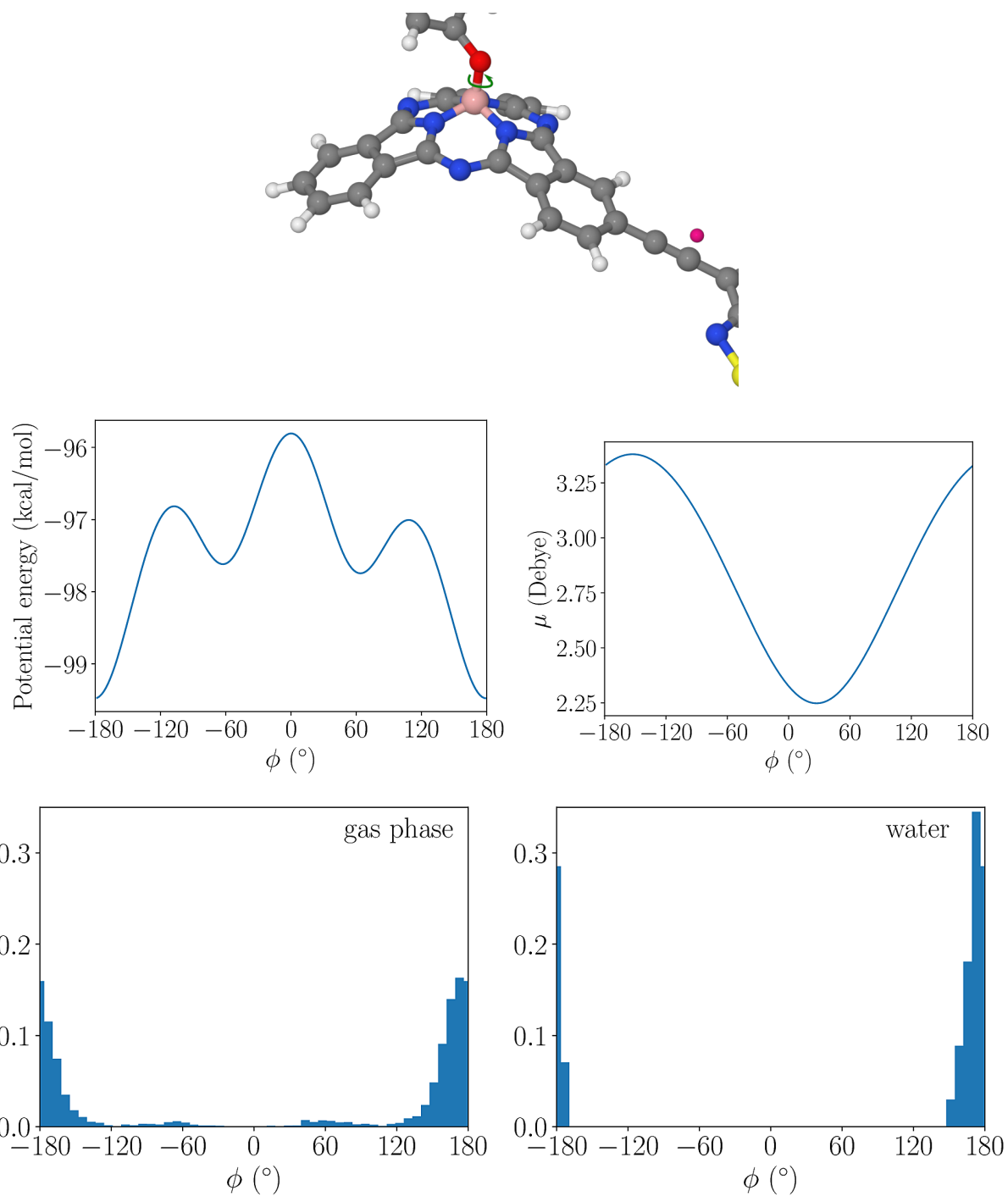


Figure S16: Top: Illustration the dihedral rotation  $D4$  between fragments 3 and 4; Middle left: The total energy profile involved in this rotation (N25-B27-O28-C29) for the isolated SubPC; Middle Right: Dipole moment  $\mu$  as a function of the rotation; Bottom left: Dihedral distribution obtained with the CBMC simulation of the isolated SubPC (gas phase); and Bottom right: Distribution obtained with the CBMC simulation of SubPC in water.

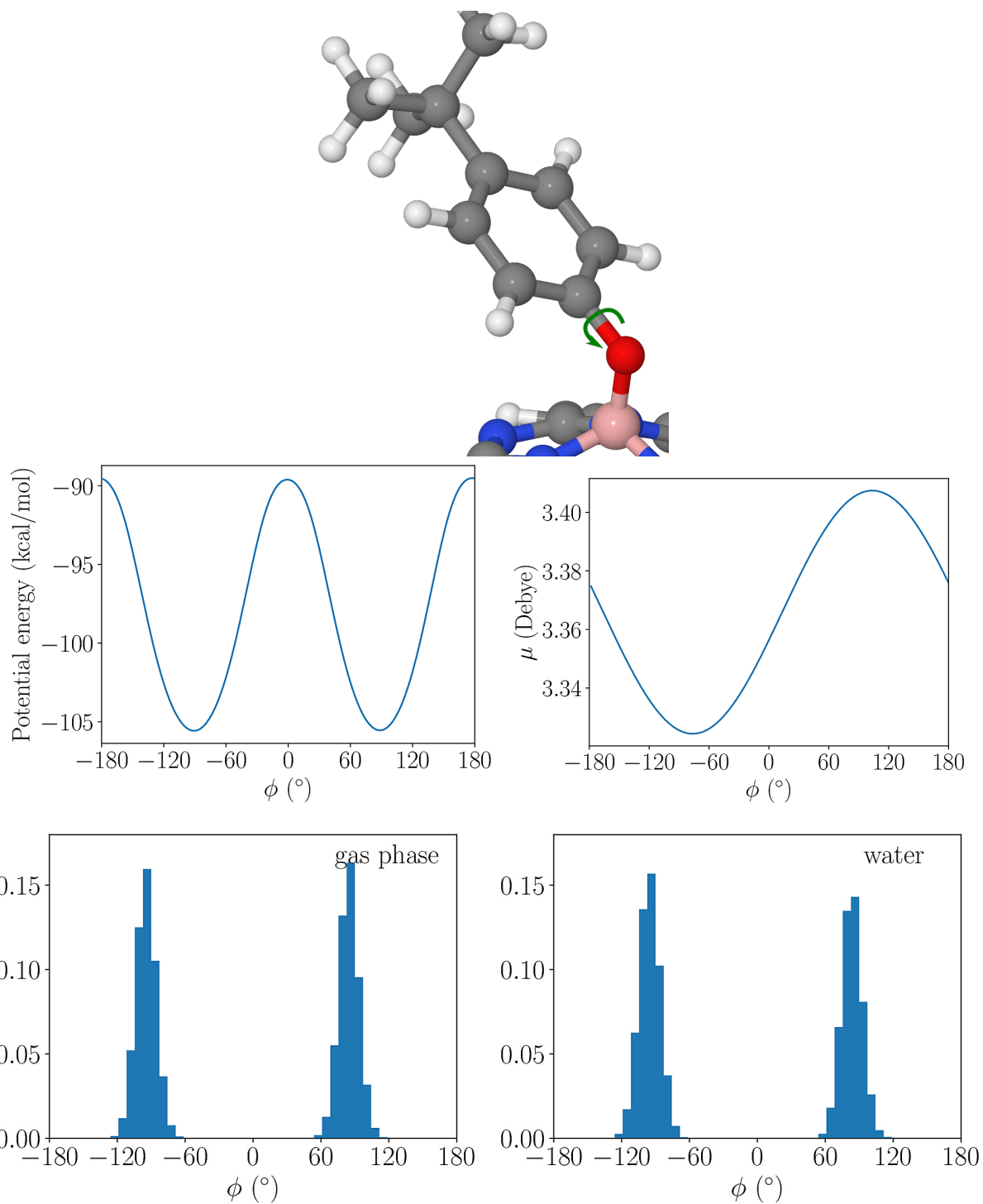


Figure S17: Top: Illustration the dihedral rotation  $D5$  between fragments 4 and 5; Middle left: The total energy profile involved in this rotation (B27-O28-C29-C30) for the isolated SubPC; Middle Right: Dipole moment  $\mu$  as a function of the rotation; Bottom left: Dihedral distribution obtained with the CBMC simulation of the isolated SubPC (gas phase); and Bottom right: Distribution obtained with the CBMC simulation of SubPC in water.



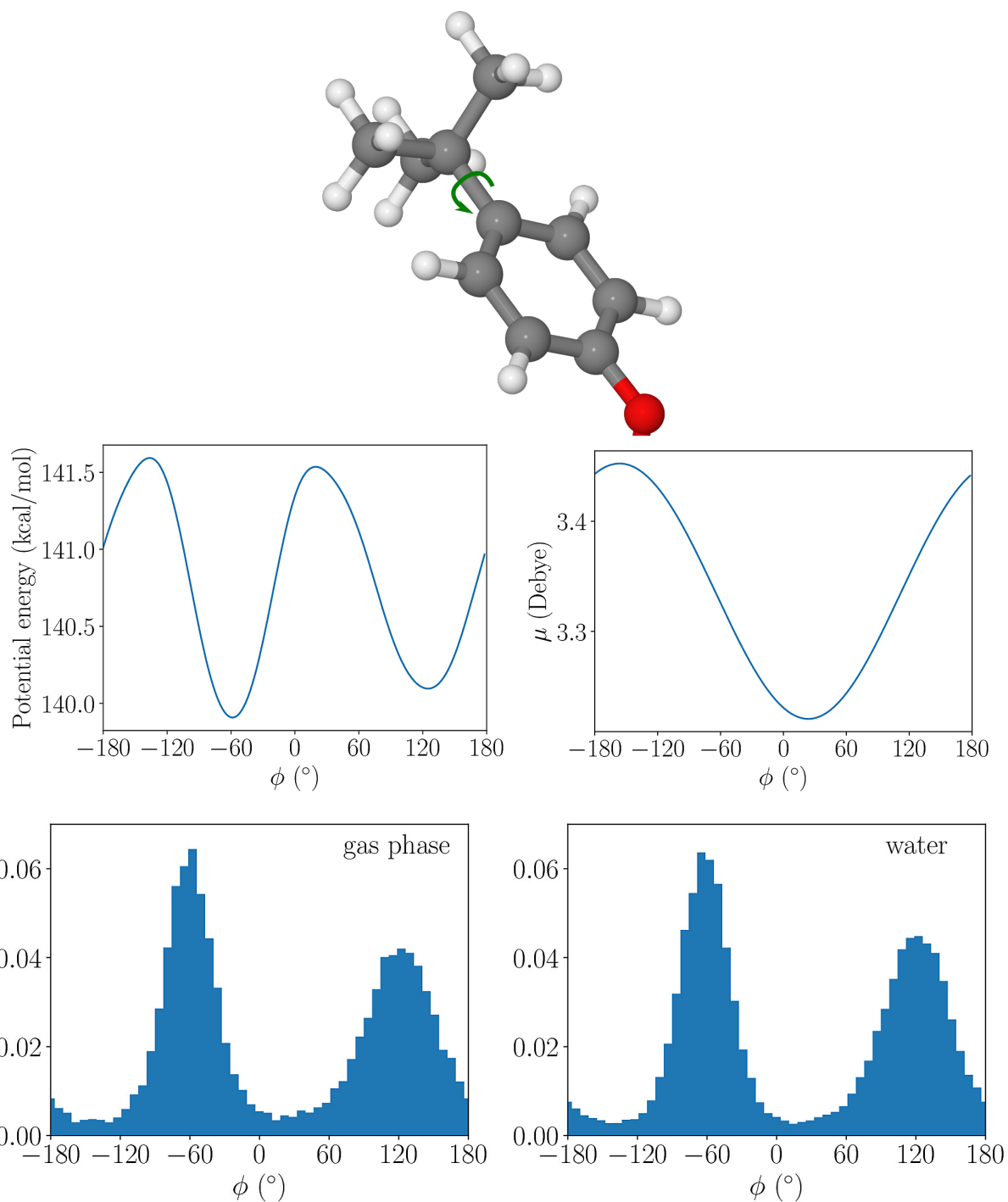


Figure S18: Top: Illustration the dihedral rotation  $D6$  between fragments 5 and 6; Middle left: The total energy profile involved in this rotation (C31-C32-C56-C61) for the isolated SubPC; Middle Right: Dipole moment  $\mu$  as a function of the rotation; Bottom left: Dihedral distribution obtained with the CBMC simulation of the isolated SubPC (gas phase); and Bottom right: Distribution obtained with the CBMC simulation of SubPC in water.

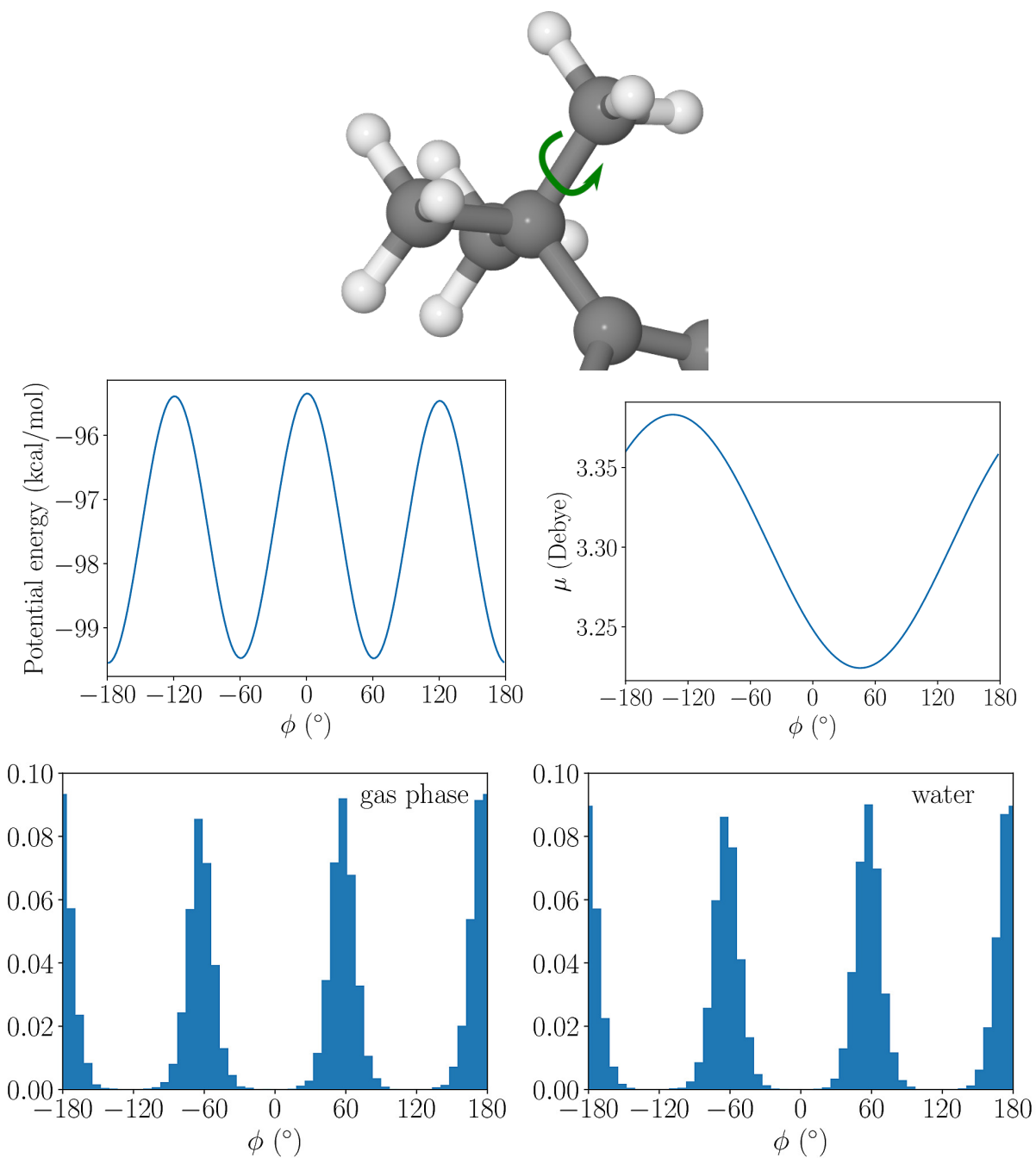


Figure S19: Top: Illustration the dihedral rotation  $D7$  between fragments 6 and 7; Middle left: The total energy profile involved in this rotation (C32-C56-C57-H82) for the isolated SubPC; Middle Right: Dipole moment  $\mu$  as a function of the rotation; Bottom left: Dihedral distribution obtained with the CBMC simulation of the isolated SubPC (gas phase); and Bottom right: Distribution obtained with the CBMC simulation of SubPC in water.

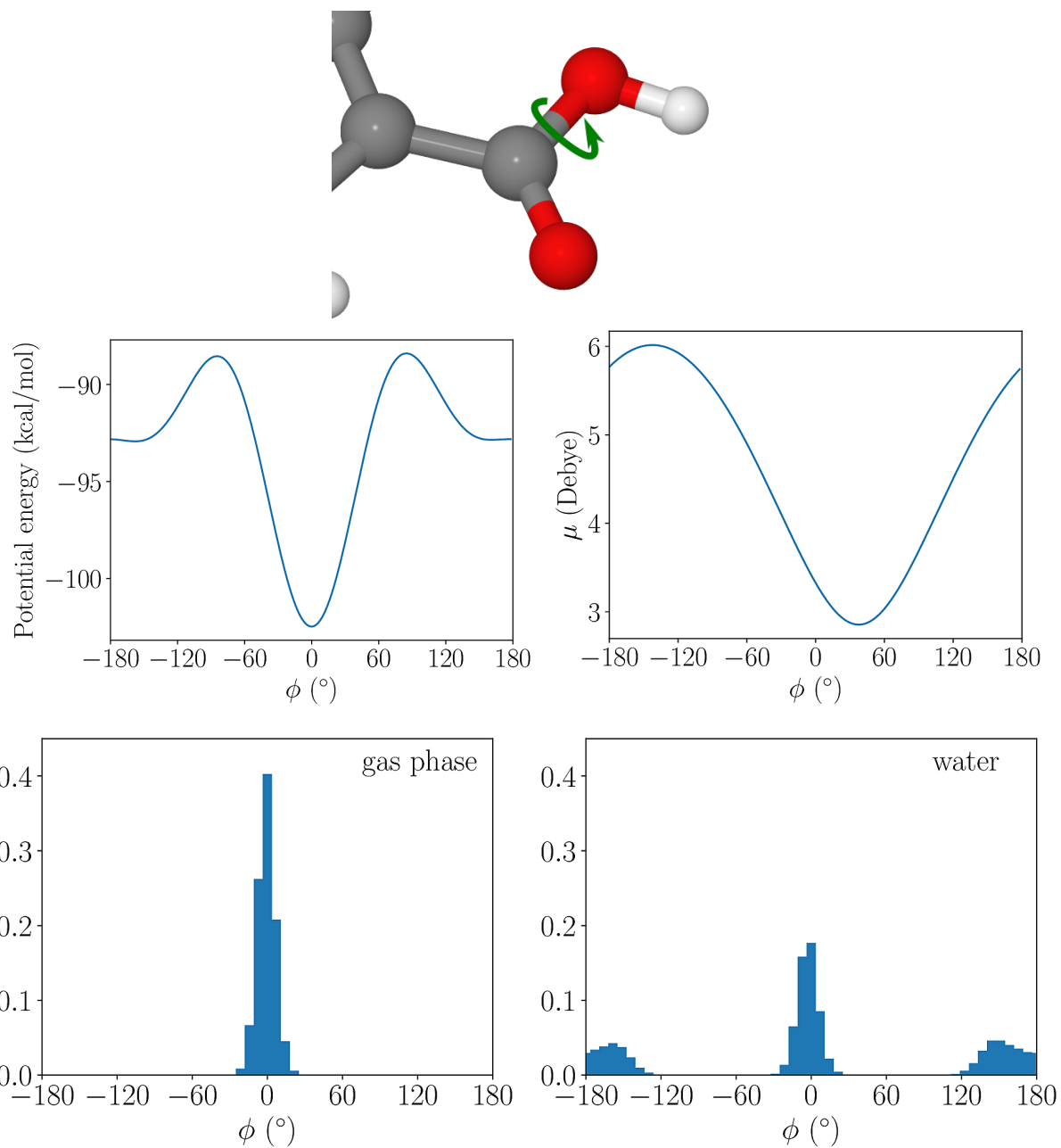


Figure S20: Top: Illustration the dihedral rotation  $D8$  between fragments 8 and 9; Middle left: The total energy profile involved in this rotation (O62-C58-O59-H91) for the isolated SubPC; Middle Right: Dipole moment  $\mu$  as a function of the rotation; Bottom left: Dihedral distribution obtained with the CBMC simulation of the isolated SubPC (gas phase); and Bottom right: Distribution obtained with the CBMC simulation of SubPC in water.

## SI 5: Example input files

Below we provide some example input files, which were used to produce the data reported in this work. The `.txt` files contain the initial geometry of each type of molecules with Cartesian coordinates of the atoms  $\{x_i, y_i, z_i\}$  in Å, and also the nonbonded parameters: the atomic partial charges  $\{q_i\}$  in  $e$  and the Lennard-Jones parameters  $\{\epsilon_i\}$  and  $\{\sigma_i\}$  in kcal/mol and Å, respectively. The topology, with the intramolecular potential, is defined in the `.dfr` file. The input files for the thermalization and CBMC simulation are passed to DICE via shell redirection of input files with the `<` operator.

These input files were prepared using DICEtools (<https://github.com/hmcezar/dicetools>), which provides tools to generate input files from standard chemical structure information and conversion between DICE and GROMACS[12] input files.

### SI 5.1: Octane

Geometry and nonbonded parameters: octane.txt

```
2
26      octane generated with gromacs2dice
1 6      -5.2546      0.1842      -0.0141      -0.18      0.0660      3.5000
1 6      -4.1421      1.2201      0.0053      -0.12      0.0660      3.5000
2 1      -5.1657      -0.4749      -0.8833      0.06      0.0300      2.5000
2 1      -6.2303      0.6785      -0.0608      0.06      0.0300      2.5000
2 1      -5.2301      -0.4321      0.8902      0.06      0.0300      2.5000
1 6      -2.7591      0.5659      -0.0193      -0.12      0.0660      3.5000
2 1      -4.2479      1.8431      0.9011      0.06      0.0300      2.5000
2 1      -4.2527      1.8812      -0.8623      0.06      0.0300      2.5000
1 6      -1.6537      1.6211      0.0364      -0.12      0.0660      3.5000
2 1      -2.6535      -0.0317      -0.9327      0.06      0.0300      2.5000
2 1      -2.6585      -0.1197      0.8306      0.06      0.0300      2.5000
1 6      -0.2605      0.9917      -0.0258      -0.12      0.0660      3.5000
2 1      -1.7512      2.2029      0.9611      0.06      0.0300      2.5000
2 1      -1.7747      2.3212      -0.7993      0.06      0.0300      2.5000
1 6      0.8250      2.0688      0.0287      -0.12      0.0660      3.5000
2 1      -0.1591      0.4123      -0.9515      0.06      0.0300      2.5000
2 1      -0.1315      0.2940      0.8104      0.06      0.0300      2.5000
1 6      2.2274      1.4681      -0.0556      -0.12      0.0660      3.5000
2 1      0.7271      2.6394      0.9603      0.06      0.0300      2.5000
2 1      0.6808      2.7752      -0.7981      0.06      0.0300      2.5000
1 6      3.2935      2.5523      -0.0138      -0.18      0.0660      3.5000
2 1      2.3332      0.8950      -0.9841      0.06      0.0300      2.5000
2 1      2.3873      0.7725      0.7763      0.06      0.0300      2.5000
2 1      3.1709      3.2551      -0.8444      0.06      0.0300      2.5000
2 1      4.2910      2.1087      -0.0891      0.06      0.0300      2.5000
2 1      3.2422      3.1166      0.9230      0.06      0.0300      2.5000
5 Cloroformio OPLS/AA JPOC, 10, 563, 1997      Densidade= 1.45g/cm3
1 6      0.000000      0.000000      0.460827      -0.063      0.066      3.50
2 1      0.000000      0.000000      1.545977      0.216      0.030      2.50
3 17     0.000000      1.704389      -0.084528      -0.051      0.300      3.47
3 17     1.476044      -0.852194      -0.084528      -0.051      0.300      3.47
3 17     -1.476044      -0.852194      -0.084528      -0.051      0.300      3.47
$end
```

Topology: octane.dfr

```
$atoms fragments
1      [ 1      2      5      4      3 ]      F
2      [ 2      6      1      7      8 ]      F
3      [ 6      9      2      11     10 ]      F
4      [ 9      12     6      13     14 ]      F
5      [ 12     15     9      17     16 ]      F
6      [ 15     18     12     19     20 ]      F
7      [ 18     21     15     23     22 ]      F
8      [ 21     18     26     25     24 ]      F
$end atoms fragments

$fragment connection
1      2
2      3
3      4
```

4 5  
5 6  
6 7  
7 8

\$send fragment connection

\$bond

1 5	340.0	1.09
1 4	340.0	1.09
1 3	340.0	1.09
1 2	268.0	1.52
2 8	340.0	1.1
2 7	340.0	1.1
2 6	268.0	1.53
6 11	340.0	1.1
6 10	340.0	1.1
6 9	268.0	1.53
9 14	340.0	1.1
9 13	340.0	1.1
9 12	268.0	1.53
12 17	340.0	1.1
12 16	340.0	1.1
12 15	268.0	1.53
15 20	340.0	1.1
15 19	340.0	1.1
15 18	268.0	1.53
18 23	340.0	1.1
18 22	340.0	1.1
18 21	268.0	1.52
21 26	340.0	1.1
21 25	340.0	1.09
21 24	340.0	1.09

\$end bond

\$angle

1 2 8	harmonic	37.5	109.081
1 2 7	harmonic	37.5	109.06
1 2 6	harmonic	58.35	111.727
2 1 5	harmonic	37.5	110.885
2 1 4	harmonic	37.5	110.147
2 1 3	harmonic	37.5	111.143
2 6 11	harmonic	37.5	109.778
2 6 10	harmonic	37.5	109.421
2 6 9	harmonic	58.35	110.966
3 1 5	harmonic	33.0	108.373
3 1 4	harmonic	33.0	108.103
4 1 5	harmonic	33.0	108.086
6 2 8	harmonic	37.5	109.692
6 2 7	harmonic	37.5	110.065
6 9 14	harmonic	37.5	109.479
6 9 13	harmonic	37.5	109.421
6 9 12	harmonic	58.35	111.916
7 2 8	harmonic	33.0	107.098
9 6 11	harmonic	37.5	109.703
9 6 10	harmonic	37.5	109.688
9 12 17	harmonic	37.5	109.743
9 12 16	harmonic	37.5	109.6
9 12 15	harmonic	58.35	110.805
10 6 11	harmonic	33.0	107.207
12 9 14	harmonic	37.5	109.394
12 9 13	harmonic	37.5	109.431
12 15 20	harmonic	37.5	109.447
12 15 19	harmonic	37.5	109.467
12 15 18	harmonic	58.35	111.834
13 9 14	harmonic	33.0	107.078
15 12 17	harmonic	37.5	109.709
15 12 16	harmonic	37.5	109.719
15 18 23	harmonic	37.5	109.962
15 18 22	harmonic	37.5	109.974
15 18 21	harmonic	58.35	111.206
16 12 17	harmonic	33.0	107.192
18 15 20	harmonic	37.5	109.374
18 15 19	harmonic	37.5	109.506
18 21 26	harmonic	37.5	110.964
18 21 25	harmonic	37.5	110.415
18 21 24	harmonic	37.5	110.965
19 15 20	harmonic	33.0	107.096
21 18 23	harmonic	37.5	109.204
21 18 22	harmonic	37.5	109.151
22 18 23	harmonic	33.0	107.252
24 21 26	harmonic	33.0	108.18
24 21 25	harmonic	33.0	108.096
25 21 26	harmonic	33.0	108.113

\$end angle

\$dihedral

5 1 2 8	OPLS	-0.0	-0.0	0.3	0.0	0.0	0.0	0.0
---------	------	------	------	-----	-----	-----	-----	-----

4 1 2 8	OPLS	-0.0	-0.0	0.3	0.0	0.0	0.0	0.0
3 1 2 8	OPLS	-0.0	-0.0	0.3	0.0	0.0	0.0	0.0
5 1 2 7	OPLS	-0.0	-0.0	0.3	0.0	0.0	0.0	0.0
4 1 2 7	OPLS	-0.0	-0.0	0.3	0.0	0.0	0.0	0.0
3 1 2 7	OPLS	-0.0	-0.0	0.3	0.0	0.0	0.0	0.0
5 1 2 6	OPLS	-0.0	-0.0	0.3	0.0	0.0	0.0	0.0
4 1 2 6	OPLS	-0.0	-0.0	0.3	0.0	0.0	0.0	0.0
3 1 2 6	OPLS	-0.0	-0.0	0.3	0.0	0.0	0.0	0.0
1 2 6 11	OPLS	-0.0	-0.0	0.3	0.0	0.0	0.0	0.0
8 2 6 11	OPLS	-0.0	-0.0	0.3	0.0	0.0	0.0	0.0
7 2 6 11	OPLS	-0.0	-0.0	0.3	0.0	0.0	0.0	0.0
1 2 6 10	OPLS	-0.0	-0.0	0.3	0.0	0.0	0.0	0.0
8 2 6 10	OPLS	-0.0	-0.0	0.3	0.0	0.0	0.0	0.0
7 2 6 10	OPLS	-0.0	-0.0	0.3	0.0	0.0	0.0	0.0
1 2 6 9	OPLS	1.3	-0.05	0.2	0.0	0.0	0.0	0.0
8 2 6 9	OPLS	-0.0	-0.0	0.3	0.0	0.0	0.0	0.0
7 2 6 9	OPLS	-0.0	-0.0	0.3	0.0	0.0	0.0	0.0
2 6 9 14	OPLS	-0.0	-0.0	0.3	0.0	0.0	0.0	0.0
11 6 9 14	OPLS	-0.0	-0.0	0.3	0.0	0.0	0.0	0.0
10 6 9 14	OPLS	-0.0	-0.0	0.3	0.0	0.0	0.0	0.0
2 6 9 13	OPLS	-0.0	-0.0	0.3	0.0	0.0	0.0	0.0
11 6 9 13	OPLS	-0.0	-0.0	0.3	0.0	0.0	0.0	0.0
10 6 9 13	OPLS	-0.0	-0.0	0.3	0.0	0.0	0.0	0.0
2 6 9 12	OPLS	1.3	-0.05	0.2	0.0	0.0	0.0	0.0
11 6 9 12	OPLS	-0.0	-0.0	0.3	0.0	0.0	0.0	0.0
10 6 9 12	OPLS	-0.0	-0.0	0.3	0.0	0.0	0.0	0.0
6 9 12 17	OPLS	-0.0	-0.0	0.3	0.0	0.0	0.0	0.0
14 9 12 17	OPLS	-0.0	-0.0	0.3	0.0	0.0	0.0	0.0
13 9 12 17	OPLS	-0.0	-0.0	0.3	0.0	0.0	0.0	0.0
6 9 12 16	OPLS	-0.0	-0.0	0.3	0.0	0.0	0.0	0.0
14 9 12 16	OPLS	-0.0	-0.0	0.3	0.0	0.0	0.0	0.0
13 9 12 16	OPLS	-0.0	-0.0	0.3	0.0	0.0	0.0	0.0
6 9 12 15	OPLS	1.3	-0.05	0.2	0.0	0.0	0.0	0.0
14 9 12 15	OPLS	-0.0	-0.0	0.3	0.0	0.0	0.0	0.0
13 9 12 15	OPLS	-0.0	-0.0	0.3	0.0	0.0	0.0	0.0
9 12 15 20	OPLS	-0.0	-0.0	0.3	0.0	0.0	0.0	0.0
17 12 15 20	OPLS	-0.0	-0.0	0.3	0.0	0.0	0.0	0.0
16 12 15 20	OPLS	-0.0	-0.0	0.3	0.0	0.0	0.0	0.0
9 12 15 19	OPLS	-0.0	-0.0	0.3	0.0	0.0	0.0	0.0
17 12 15 19	OPLS	-0.0	-0.0	0.3	0.0	0.0	0.0	0.0
16 12 15 19	OPLS	-0.0	-0.0	0.3	0.0	0.0	0.0	0.0
9 12 15 18	OPLS	1.3	-0.05	0.2	0.0	0.0	0.0	0.0
17 12 15 18	OPLS	-0.0	-0.0	0.3	0.0	0.0	0.0	0.0
16 12 15 18	OPLS	-0.0	-0.0	0.3	0.0	0.0	0.0	0.0
12 15 18 23	OPLS	-0.0	-0.0	0.3	0.0	0.0	0.0	0.0
20 15 18 23	OPLS	-0.0	-0.0	0.3	0.0	0.0	0.0	0.0
19 15 18 23	OPLS	-0.0	-0.0	0.3	0.0	0.0	0.0	0.0
12 15 18 22	OPLS	-0.0	-0.0	0.3	0.0	0.0	0.0	0.0
20 15 18 22	OPLS	-0.0	-0.0	0.3	0.0	0.0	0.0	0.0
19 15 18 22	OPLS	-0.0	-0.0	0.3	0.0	0.0	0.0	0.0
12 15 18 21	OPLS	1.3	-0.05	0.2	0.0	0.0	0.0	0.0
20 15 18 21	OPLS	-0.0	-0.0	0.3	0.0	0.0	0.0	0.0
19 15 18 21	OPLS	-0.0	-0.0	0.3	0.0	0.0	0.0	0.0
15 18 21 26	OPLS	-0.0	-0.0	0.3	0.0	0.0	0.0	0.0
23 18 21 26	OPLS	-0.0	-0.0	0.3	0.0	0.0	0.0	0.0
22 18 21 26	OPLS	-0.0	-0.0	0.3	0.0	0.0	0.0	0.0
15 18 21 25	OPLS	-0.0	-0.0	0.3	0.0	0.0	0.0	0.0
23 18 21 25	OPLS	-0.0	-0.0	0.3	0.0	0.0	0.0	0.0
22 18 21 25	OPLS	-0.0	-0.0	0.3	0.0	0.0	0.0	0.0
15 18 21 24	OPLS	-0.0	-0.0	0.3	0.0	0.0	0.0	0.0
23 18 21 24	OPLS	-0.0	-0.0	0.3	0.0	0.0	0.0	0.0
22 18 21 24	OPLS	-0.0	-0.0	0.3	0.0	0.0	0.0	0.0

\$end dihedral

---

DICE thermalization input: octane.ter

---

```

title = octane_chloroform_therm
ljname = octane.txt
outname = outoctane
ncores = 6
init = yes
coolstep = 200
nmol = 1 1000
dens = 1.45
temp = 298.15
press = 1.0
upbuf = 100
accum = no
vstep = 25000
nstep = 4
iprint = 1
isave = 5000
irdf = 0
iratio = 10

```

```
vratio = 10
seed = 85513
nsf = 10000
sfint = 500
```

DICE CBMC simulation input: octane.in

```
title = octane_chloroform
ljname = octane.txt
outname = outoctane
ncores = 6
init = no
temp = 298.15
press = 1.0
accum = no
vstep = 125000
nstep = 4
iprint = 1
isave = 50
irdf = 5
iratio = 10
vratio = 10
seed = 208043
flex = octane
nsf = 10000
sfint = 500
equiPhi = yes
ntrialPhi = 18
pcbmc = 0.7
dielectric = 4.81
upbuf = 100
sampling = 2
```

## SI 5.2: neopentane

Geometry and nonbonded parameters: neopentane.txt

```
1
17      neopentane generated with gromacs2dice
1 6      1.0000      1.0000      0.0000      -0.1800      0.0660      3.5000
1 6      -0.5400      1.0000      0.0000      0.0000      0.0660      3.5000
1 6      -1.0400      1.0000      1.4500      -0.1800      0.0660      3.5000
1 6      -1.0400      2.2600      -0.7200      -0.1800      0.0660      3.5000
1 6      -1.0400      -0.2600      -0.7200      -0.1800      0.0660      3.5000
2 1      1.4000      1.8900      0.5100      0.0600      0.0300      2.5000
2 1      1.4000      1.0000      -1.0200      0.0600      0.0300      2.5000
2 1      1.4000      0.1200      0.5100      0.0600      0.0300      2.5000
2 1      -0.6900      1.8900      1.9900      0.0600      0.0300      2.5000
2 1      -0.6900      0.1200      1.9900      0.0600      0.0300      2.5000
2 1      -2.1400      1.0000      1.4800      0.0600      0.0300      2.5000
2 1      -0.6900      3.1700      -0.2300      0.0600      0.0300      2.5000
2 1      -2.1400      2.2800      -0.7400      0.0600      0.0300      2.5000
2 1      -0.6900      2.2800      -1.7600      0.0600      0.0300      2.5000
2 1      -0.6900      -1.1700      -0.2300      0.0600      0.0300      2.5000
2 1      -0.6900      -0.2800      -1.7600      0.0600      0.0300      2.5000
2 1      -2.1400      -0.2800      -0.7400      0.0600      0.0300      2.5000
$end
```

Topology: neopentane.dfr

```
$atoms fragments
1      [ 1      2      6      8      7      ] F
2      [ 2      3      5      4      1      ] F
3      [ 3      2      9      10     11     ] F
4      [ 4      2      12     13     14     ] F
5      [ 5      2      15     17     16     ] F
$end atoms fragments

$fragment connection
1      2
2      4
2      5
2      3
$end fragment connection

$bond
2 1      268.0      1.529
```

3 2	268.0	1.529
4 2	268.0	1.529
5 2	268.0	1.529
6 1	340.0	1.09
7 1	340.0	1.09
8 1	340.0	1.09
9 3	340.0	1.09
10 3	340.0	1.09
11 3	340.0	1.09
12 4	340.0	1.09
13 4	340.0	1.09
14 4	340.0	1.09
15 5	340.0	1.09
16 5	340.0	1.09
17 5	340.0	1.09

\$end bond

\$angle

1 2 3	harmonic	58.35	112.7
1 2 4	harmonic	58.35	112.7
1 2 5	harmonic	58.35	112.7
2 1 6	harmonic	37.5	110.7
2 1 7	harmonic	37.5	110.7
2 1 8	harmonic	37.5	110.7
2 3 9	harmonic	37.5	110.7
2 3 10	harmonic	37.5	110.7
2 3 11	harmonic	37.5	110.7
2 4 12	harmonic	37.5	110.7
2 4 13	harmonic	37.5	110.7
2 4 14	harmonic	37.5	110.7
2 5 15	harmonic	37.5	110.7
2 5 16	harmonic	37.5	110.7
2 5 17	harmonic	37.5	110.7
15 5 16	harmonic	33.0	107.8
13 4 14	harmonic	33.0	107.8
15 5 17	harmonic	33.0	107.8
10 3 11	harmonic	33.0	107.8
16 5 17	harmonic	33.0	107.8
3 2 4	harmonic	58.35	112.7
9 3 10	harmonic	33.0	107.8
3 2 5	harmonic	58.35	112.7
4 2 5	harmonic	58.35	112.7
12 4 13	harmonic	33.0	107.8
9 3 11	harmonic	33.0	107.8
7 1 8	harmonic	33.0	107.8
6 1 7	harmonic	33.0	107.8
12 4 14	harmonic	33.0	107.8
6 1 8	harmonic	33.0	107.8

\$end angle

\$dihedral

13 4 2 3	OPLS	-0.0	-0.0	0.3	0.0	0.0	0.0
9 3 2 4	OPLS	-0.0	-0.0	0.3	0.0	0.0	0.0
15 5 2 4	OPLS	-0.0	-0.0	0.3	0.0	0.0	0.0
17 5 2 4	OPLS	-0.0	-0.0	0.3	0.0	0.0	0.0
16 5 2 3	OPLS	-0.0	-0.0	0.3	0.0	0.0	0.0
17 5 2 3	OPLS	-0.0	-0.0	0.3	0.0	0.0	0.0
16 5 2 4	OPLS	-0.0	-0.0	0.3	0.0	0.0	0.0
9 3 2 5	OPLS	-0.0	-0.0	0.3	0.0	0.0	0.0
8 1 2 3	OPLS	-0.0	-0.0	0.3	0.0	0.0	0.0
6 1 2 5	OPLS	-0.0	-0.0	0.3	0.0	0.0	0.0
7 1 2 4	OPLS	-0.0	-0.0	0.3	0.0	0.0	0.0
12 4 2 5	OPLS	-0.0	-0.0	0.3	0.0	0.0	0.0
10 3 2 1	OPLS	-0.0	-0.0	0.3	0.0	0.0	0.0
13 4 2 1	OPLS	-0.0	-0.0	0.3	0.0	0.0	0.0
10 3 2 5	OPLS	-0.0	-0.0	0.3	0.0	0.0	0.0
11 3 2 4	OPLS	-0.0	-0.0	0.3	0.0	0.0	0.0
16 5 2 1	OPLS	-0.0	-0.0	0.3	0.0	0.0	0.0
12 4 2 3	OPLS	-0.0	-0.0	0.3	0.0	0.0	0.0
10 3 2 4	OPLS	-0.0	-0.0	0.3	0.0	0.0	0.0
17 5 2 1	OPLS	-0.0	-0.0	0.3	0.0	0.0	0.0
14 4 2 3	OPLS	-0.0	-0.0	0.3	0.0	0.0	0.0
14 4 2 5	OPLS	-0.0	-0.0	0.3	0.0	0.0	0.0
11 3 2 5	OPLS	-0.0	-0.0	0.3	0.0	0.0	0.0
6 1 2 3	OPLS	-0.0	-0.0	0.3	0.0	0.0	0.0
9 3 2 1	OPLS	-0.0	-0.0	0.3	0.0	0.0	0.0
12 4 2 1	OPLS	-0.0	-0.0	0.3	0.0	0.0	0.0
8 1 2 5	OPLS	-0.0	-0.0	0.3	0.0	0.0	0.0
11 3 2 1	OPLS	-0.0	-0.0	0.3	0.0	0.0	0.0
15 5 2 1	OPLS	-0.0	-0.0	0.3	0.0	0.0	0.0
7 1 2 5	OPLS	-0.0	-0.0	0.3	0.0	0.0	0.0
8 1 2 4	OPLS	-0.0	-0.0	0.3	0.0	0.0	0.0
7 1 2 3	OPLS	-0.0	-0.0	0.3	0.0	0.0	0.0
6 1 2 4	OPLS	-0.0	-0.0	0.3	0.0	0.0	0.0
13 4 2 5	OPLS	-0.0	-0.0	0.3	0.0	0.0	0.0
15 5 2 3	OPLS	-0.0	-0.0	0.3	0.0	0.0	0.0
14 4 2 1	OPLS	-0.0	-0.0	0.3	0.0	0.0	0.0



\$end dihedral

DICE CBMC simulation input: neopentane.in

```
title = neopentane_gas
ljname = neopentane.txt
outname = outneopentane
ncores = 4
init = yes
coolstep = 0
nmol = 1
dens = 0.001
temp = 298.15
press = 1.0
upbuf = 99999999
accum = no
vstep = 0
nstep = 10000000
iprint = 1
isave = 100
irdf = 0
iratio = 10
vratio = 10
seed = 70016
flex = neopentane
pcbmc = 1.0
equiphi = yes
ntrialphi = 12
nsf = 10000
sfint = 500
```

## SI 5.3: 4-ethylheptane

Geometry and nonbonded parameters: 4ethylheptane.txt

```
1
29      4ethylheptane generated with gromacs2dice
1 6      1.0000      1.0000      0.0000      -0.1800      0.0660      3.5000
1 6      -0.5200      1.0000      0.0000      -0.1200      0.0660      3.5000
1 6      -1.0600      1.0000      1.4300      -0.1200      0.0660      3.5000
1 6      -2.6000      1.0600      1.5400      -0.0600      0.0660      3.5000
1 6      -3.3200      -0.0600      0.7600      -0.1200      0.0660      3.5000
1 6      -3.0600      -1.4700      1.2600      -0.1800      0.0660      3.5000
1 6      -3.0600      1.0700      3.0200      -0.1200      0.0660      3.5000
1 6      -2.5600      2.2800      3.8100      -0.1200      0.0660      3.5000
1 6      -3.0400      2.2400      5.2600      -0.1800      0.0660      3.5000
2 1      1.3800      1.0000      -1.0300      0.0600      0.0300      2.5000
2 1      1.3900      0.1100      0.5100      0.0600      0.0300      2.5000
2 1      1.4000      1.8900      0.5100      0.0600      0.0300      2.5000
2 1      -0.8600      0.1200      -0.5500      0.0600      0.0300      2.5000
2 1      -0.8800      1.8800      -0.5400      0.0600      0.0300      2.5000
2 1      -0.6300      1.8700      1.9300      0.0600      0.0300      2.5000
2 1      -0.6900      0.1200      1.9700      0.0600      0.0300      2.5000
2 1      -2.9200      2.0100      1.0800      0.0600      0.0300      2.5000
2 1      -3.0500      -0.0100      -0.3000      0.0600      0.0300      2.5000
2 1      -4.4100      0.1200      0.7900      0.0600      0.0300      2.5000
2 1      -2.0000      -1.6600      1.4500      0.0600      0.0300      2.5000
2 1      -3.4000      -2.2000      0.5200      0.0600      0.0300      2.5000
2 1      -3.6200      -1.6700      2.1800      0.0600      0.0300      2.5000
2 1      -2.7200      0.1600      3.5100      0.0600      0.0300      2.5000
2 1      -4.1600      1.0600      3.0500      0.0600      0.0300      2.5000
2 1      -2.9100      3.2100      3.3400      0.0600      0.0300      2.5000
2 1      -1.4700      2.3100      3.8300      0.0600      0.0300      2.5000
2 1      -4.1300      2.2500      5.3100      0.0600      0.0300      2.5000
2 1      -2.6600      3.1100      5.8000      0.0600      0.0300      2.5000
2 1      -2.6700      1.3400      5.7600      0.0600      0.0300      2.5000
$end
```

Topology: 4ethylheptane.dfr

```
$atoms fragments
1      [ 1      2      11      12      10      ] M
2      [ 2      3      1      14      13      ] M
3      [ 3      4      2      16      15      ] M
4      [ 4      7      5      3      17      ] M
5      [ 5      6      4      19      18      ] M
6      [ 6      5      22      20      21      ] M
```

```

7      [ 7      8      4      23      24      ] M
8      [ 8      9      7      26      25      ] M
9      [ 9      8      28     29      27      ] M

```

\$end atoms fragments

\$fragment connection

```

1      2
2      3
3      4
4      5
4      7
5      6
7      8
8      9

```

\$end fragment connection

\$bond

```

2 1      268.0    1.529
3 2      268.0    1.529
4 3      268.0    1.529
5 4      268.0    1.529
6 5      268.0    1.529
7 4      268.0    1.529
8 7      268.0    1.529
9 8      268.0    1.529
10 1     340.0     1.09
11 1     340.0     1.09
12 1     340.0     1.09
13 2     340.0     1.09
14 2     340.0     1.09
15 3     340.0     1.09
16 3     340.0     1.09
17 4     340.0     1.09
18 5     340.0     1.09
19 5     340.0     1.09
20 6     340.0     1.09
21 6     340.0     1.09
22 6     340.0     1.09
23 7     340.0     1.09
24 7     340.0     1.09
25 8     340.0     1.09
26 8     340.0     1.09
27 9     340.0     1.09
28 9     340.0     1.09
29 9     340.0     1.09

```

\$end bond

\$angle

```

1 2 3     harmonic    58.35    112.7
2 3 4     harmonic    58.35    112.7
3 4 5     harmonic    58.35    112.7
4 5 6     harmonic    58.35    112.7
3 4 7     harmonic    58.35    112.7
4 7 8     harmonic    58.35    112.7
7 8 9     harmonic    58.35    112.7
2 1 10    harmonic    37.5     110.7
2 1 11    harmonic    37.5     110.7
2 1 12    harmonic    37.5     110.7
1 2 13    harmonic    37.5     110.7
1 2 14    harmonic    37.5     110.7
2 3 15    harmonic    37.5     110.7
2 3 16    harmonic    37.5     110.7
3 4 17    harmonic    37.5     110.7
4 5 18    harmonic    37.5     110.7
4 5 19    harmonic    37.5     110.7
5 6 20    harmonic    37.5     110.7
5 6 21    harmonic    37.5     110.7
5 6 22    harmonic    37.5     110.7
4 7 23    harmonic    37.5     110.7
4 7 24    harmonic    37.5     110.7
7 8 25    harmonic    37.5     110.7
7 8 26    harmonic    37.5     110.7
8 9 27    harmonic    37.5     110.7
8 9 28    harmonic    37.5     110.7
8 9 29    harmonic    37.5     110.7
23 7 24    harmonic    33.0     107.8
9 8 25    harmonic    37.5     110.7
3 2 14    harmonic    37.5     110.7
13 2 14    harmonic    33.0     107.8
20 6 21    harmonic    33.0     107.8
5 4 7     harmonic    58.35    112.7
21 6 22    harmonic    33.0     107.8
20 6 22    harmonic    33.0     107.8
6 5 19    harmonic    37.5     110.7
28 9 29    harmonic    33.0     107.8
15 3 16    harmonic    33.0     107.8
8 7 23    harmonic    37.5     110.7

```

27 9 29	harmonic	33.0	107.8
11 1 12	harmonic	33.0	107.8
7 4 17	harmonic	37.5	110.7
25 8 26	harmonic	33.0	107.8
27 9 28	harmonic	33.0	107.8
10 1 12	harmonic	33.0	107.8
10 1 11	harmonic	33.0	107.8
3 2 13	harmonic	37.5	110.7
18 5 19	harmonic	33.0	107.8
9 8 26	harmonic	37.5	110.7
4 3 16	harmonic	37.5	110.7
8 7 24	harmonic	37.5	110.7
4 3 15	harmonic	37.5	110.7
6 5 18	harmonic	37.5	110.7
5 4 17	harmonic	37.5	110.7

\$end angle

\$dihedral

4 3 2 1	OPLS	1.3	-0.05	0.2	0.0	0.0	0.0
7 4 3 2	OPLS	1.3	-0.05	0.2	0.0	0.0	0.0
8 7 4 5	OPLS	1.3	-0.05	0.2	0.0	0.0	0.0
9 8 7 4	OPLS	1.3	-0.05	0.2	0.0	0.0	0.0
7 4 5 6	OPLS	1.3	-0.05	0.2	0.0	0.0	0.0
6 5 4 3	OPLS	1.3	-0.05	0.2	0.0	0.0	0.0
5 4 3 2	OPLS	1.3	-0.05	0.2	0.0	0.0	0.0
8 7 4 3	OPLS	1.3	-0.05	0.2	0.0	0.0	0.0
11 1 2 3	OPLS	-0.0	-0.0	0.3	0.0	0.0	0.0
24 7 8 9	OPLS	-0.0	-0.0	0.3	0.0	0.0	0.0
23 7 8 9	OPLS	-0.0	-0.0	0.3	0.0	0.0	0.0
23 7 4 3	OPLS	-0.0	-0.0	0.3	0.0	0.0	0.0
17 4 5 6	OPLS	-0.0	-0.0	0.3	0.0	0.0	0.0
29 9 8 7	OPLS	-0.0	-0.0	0.3	0.0	0.0	0.0
19 5 4 7	OPLS	-0.0	-0.0	0.3	0.0	0.0	0.0
26 8 7 4	OPLS	-0.0	-0.0	0.3	0.0	0.0	0.0
17 4 7 8	OPLS	-0.0	-0.0	0.3	0.0	0.0	0.0
25 8 7 4	OPLS	-0.0	-0.0	0.3	0.0	0.0	0.0
21 6 5 4	OPLS	-0.0	-0.0	0.3	0.0	0.0	0.0
24 7 4 5	OPLS	-0.0	-0.0	0.3	0.0	0.0	0.0
18 5 4 7	OPLS	-0.0	-0.0	0.3	0.0	0.0	0.0
12 1 2 3	OPLS	-0.0	-0.0	0.3	0.0	0.0	0.0
23 7 4 5	OPLS	-0.0	-0.0	0.3	0.0	0.0	0.0
22 6 5 4	OPLS	-0.0	-0.0	0.3	0.0	0.0	0.0
16 3 4 7	OPLS	-0.0	-0.0	0.3	0.0	0.0	0.0
19 5 4 3	OPLS	-0.0	-0.0	0.3	0.0	0.0	0.0
28 9 8 7	OPLS	-0.0	-0.0	0.3	0.0	0.0	0.0
14 2 3 4	OPLS	-0.0	-0.0	0.3	0.0	0.0	0.0
24 7 4 3	OPLS	-0.0	-0.0	0.3	0.0	0.0	0.0
13 2 3 4	OPLS	-0.0	-0.0	0.3	0.0	0.0	0.0
15 3 2 1	OPLS	-0.0	-0.0	0.3	0.0	0.0	0.0
20 6 5 4	OPLS	-0.0	-0.0	0.3	0.0	0.0	0.0
10 1 2 3	OPLS	-0.0	-0.0	0.3	0.0	0.0	0.0
18 5 4 3	OPLS	-0.0	-0.0	0.3	0.0	0.0	0.0
17 4 3 2	OPLS	-0.0	-0.0	0.3	0.0	0.0	0.0
16 3 4 5	OPLS	-0.0	-0.0	0.3	0.0	0.0	0.0
16 3 2 1	OPLS	-0.0	-0.0	0.3	0.0	0.0	0.0
27 9 8 7	OPLS	-0.0	-0.0	0.3	0.0	0.0	0.0
15 3 4 5	OPLS	-0.0	-0.0	0.3	0.0	0.0	0.0
15 3 4 7	OPLS	-0.0	-0.0	0.3	0.0	0.0	0.0
18 5 4 17	OPLS	-0.0	-0.0	0.3	0.0	0.0	0.0
14 2 1 12	OPLS	-0.0	-0.0	0.3	0.0	0.0	0.0
15 3 2 13	OPLS	-0.0	-0.0	0.3	0.0	0.0	0.0
29 9 8 25	OPLS	-0.0	-0.0	0.3	0.0	0.0	0.0
16 3 2 14	OPLS	-0.0	-0.0	0.3	0.0	0.0	0.0
22 6 5 18	OPLS	-0.0	-0.0	0.3	0.0	0.0	0.0
13 2 1 10	OPLS	-0.0	-0.0	0.3	0.0	0.0	0.0
27 9 8 26	OPLS	-0.0	-0.0	0.3	0.0	0.0	0.0
23 7 4 17	OPLS	-0.0	-0.0	0.3	0.0	0.0	0.0
17 4 3 16	OPLS	-0.0	-0.0	0.3	0.0	0.0	0.0
20 6 5 18	OPLS	-0.0	-0.0	0.3	0.0	0.0	0.0
27 9 8 25	OPLS	-0.0	-0.0	0.3	0.0	0.0	0.0
14 2 1 10	OPLS	-0.0	-0.0	0.3	0.0	0.0	0.0
29 9 8 26	OPLS	-0.0	-0.0	0.3	0.0	0.0	0.0
24 7 4 17	OPLS	-0.0	-0.0	0.3	0.0	0.0	0.0
17 4 3 15	OPLS	-0.0	-0.0	0.3	0.0	0.0	0.0
16 3 2 13	OPLS	-0.0	-0.0	0.3	0.0	0.0	0.0
25 8 7 23	OPLS	-0.0	-0.0	0.3	0.0	0.0	0.0
15 3 2 14	OPLS	-0.0	-0.0	0.3	0.0	0.0	0.0
22 6 5 19	OPLS	-0.0	-0.0	0.3	0.0	0.0	0.0
25 8 7 24	OPLS	-0.0	-0.0	0.3	0.0	0.0	0.0
28 9 8 25	OPLS	-0.0	-0.0	0.3	0.0	0.0	0.0
20 6 5 19	OPLS	-0.0	-0.0	0.3	0.0	0.0	0.0
21 6 5 18	OPLS	-0.0	-0.0	0.3	0.0	0.0	0.0
13 2 1 12	OPLS	-0.0	-0.0	0.3	0.0	0.0	0.0
14 2 1 11	OPLS	-0.0	-0.0	0.3	0.0	0.0	0.0
21 6 5 19	OPLS	-0.0	-0.0	0.3	0.0	0.0	0.0
19 5 4 17	OPLS	-0.0	-0.0	0.3	0.0	0.0	0.0
26 8 7 24	OPLS	-0.0	-0.0	0.3	0.0	0.0	0.0

```

13 2 1 11      OPLS      -0.0      -0.0      0.3      0.0      0.0      0.0
28 9 8 26      OPLS      -0.0      -0.0      0.3      0.0      0.0      0.0
26 8 7 23      OPLS      -0.0      -0.0      0.3      0.0      0.0      0.0
$end dihedral

```

---

DICE CBMC simulation input: 4ethylheptane.in

---

```

title = 4-ethylheptane_gas
ljname = 4ethylheptane.txt
outname = out4ethylheptane
ncores = 6
init = yes
coolstep = 0
nmol = 1
dens = 0.001
temp = 298.15
press = 1.0
upbuf = 99999999
accum = no
vstep = 0
nstep = 10000000
iprint = 1
isave = 100
irdf = 0
iratio = 10
vratio = 10
seed = 615330
flex = 4ethylheptane
pcbmc = 1.0
equiPhi = yes
ntrialPhi = 12
nsf = 10000
sfint = 500

```

## SI 5.4: DCE

---

Geometry and nonbonded parameters: dce.txt

---

```

1
8      DCE generated with gromacs2dice
1 17      0.055      0.0      -2.18      -0.200      0.3      3.4
2 6      -0.584      0.0      -0.494      -0.006      0.066      3.5
3 1      -1.193      0.89      -0.336      0.103      0.03      2.5
3 1      -1.193      -0.89      -0.336      0.103      0.03      2.5
2 6      0.584      0.0      0.494      -0.006      0.066      3.5
3 1      1.193      -0.89      0.336      0.103      0.03      2.5
3 1      1.193      0.89      0.336      0.103      0.03      2.5
1 17      -0.055      0.0      2.18      -0.200      0.3      3.4
$end

```

---

Topology: DCE.dfr

---

```

$atoms fragments
1      [ 1      2      5      4      3      ] F
2      [ 5      2      8      7      6      ] F
$end atoms fragments

$fragment connection
1      2
$end fragment connection

$bond
1 2      245.0      1.781
2 3      340.0      1.09
2 4      340.0      1.09
2 5      268.0      1.529
5 6      340.0      1.09
5 7      340.0      1.09
5 8      245.0      1.781
$end bond

$angle
1 2 3      harmonic      51.0      107.600
1 2 4      harmonic      51.0      107.600
1 2 5      harmonic      69.0      109.800
3 2 4      harmonic      33.0      107.800
3 2 5      harmonic      37.5      110.700

```

```

4 2 5      harmonic      37.5      110.700
2 5 6      harmonic      37.5      110.700
2 5 7      harmonic      37.5      110.700
2 5 8      harmonic      69.0      109.800
6 5 7      harmonic      33.0      107.800
6 5 8      harmonic      51.0      107.600
7 5 8      harmonic      51.0      107.600
$end angle

```

```

$dihedral
1 2 5 6      OPLS      0.0      0.0      0.4      0.0      0.0      0.0      0.0
1 2 5 7      OPLS      0.0      0.0      0.4      0.0      0.0      0.0      0.0
1 2 5 8      OPLS      -0.25     0.0      0.0      0.0      0.0      0.0      0.0
3 2 5 6      OPLS      0.0      0.0      0.318     0.0      0.0      0.0      0.0
3 2 5 7      OPLS      0.0      0.0      0.318     0.0      0.0      0.0      0.0
3 2 5 8      OPLS      0.0      0.0      0.4      0.0      0.0      0.0      0.0
4 2 5 6      OPLS      0.0      0.0      0.318     0.0      0.0      0.0      0.0
4 2 5 7      OPLS      0.0      0.0      0.318     0.0      0.0      0.0      0.0
4 2 5 8      OPLS      0.0      0.0      0.4      0.0      0.0      0.0      0.0
$end dihedral

```

---

DICE thermalization input: dce.ter

---

```

title = 12-dichloroethane_therm
ljname = DCE.txt
outname = outdce
ncores = 8
init = yes
coolstep = 250
nmol = 300
dens = 1.246
temp = 298.15
press = 1.0
accum = no
vstep = 50000
nstep = 4
iprint = 1
isave = 100
irdf = 0
iratio = 10
vratio = 10
seed = 73095

```

---

DICE CBMC simulation input: dce.in

---

```

title = 12-dichloroethane
ljname = DCE.txt
outname = outdce
ncores = 8
init = no
nmol = 300
dens = 1.246
temp = 298.15
press = 1.0
flex = DCE
ntrialphi = 32
pcbmc = 0.7
accum = yes
vstep = 500000
nstep = 4
iprint = 1
isave = 100
irdf = 5
iratio = 10
vratio = 10
seed = 62930
nsf = 10000
sfint = 500

```

## SI 5.5: SubPC

---

Geometry and nonbonded parameters: subpc.txt

---

```

2
94 subpc
1 6      12.873058      -1.455333      -0.10028      -0.107163      0.070      3.55
1 6      12.450469      -0.40574      -0.918682      -0.013610      0.070      3.55

```

1	6	11.111274	-0.040717	-0.95111	-0.244780	0.070	3.55
1	6	10.164149	-0.72226	-0.173535	0.247184	0.070	3.55
1	6	10.602464	-1.771343	0.648846	-0.205367	0.070	3.55
1	6	11.940369	-2.134176	0.685318	-0.039676	0.070	3.55
1	6	8.724595	-0.376086	-0.226869	-0.159197	0.070	3.55
1	6	7.749642	-1.342247	-0.168346	-0.100388	0.070	3.55
1	6	6.355625	-1.055152	-0.210916	-0.130470	0.070	3.55
1	6	5.871729	0.227112	-0.315144	0.001834	0.070	3.55
1	6	6.848141	1.28219	-0.375392	0.261900	0.070	3.55
1	6	8.260771	0.983688	-0.334927	0.314848	0.070	3.55
2	7	9.023488	2.073995	-0.388912	-0.417626	0.170	3.25
3	16	8.015312	3.359862	-0.488793	0.363370	0.250	3.70
2	7	6.575639	2.579246	-0.46261	-0.404432	0.170	3.25
1	6	4.479463	0.523145	-0.365382	-0.027096	0.066	3.50
1	6	3.293876	0.778781	-0.410667	-0.207739	0.066	3.50
1	6	1.901464	1.099201	-0.469095	0.264960	0.070	3.55
1	6	0.940639	0.095441	-0.322352	-0.162689	0.070	3.55
1	6	-0.403209	0.446969	-0.40799	-0.062332	0.070	3.55
1	6	-0.793382	1.800838	-0.613447	-0.095612	0.070	3.55
1	6	0.171776	2.804514	-0.730271	-0.053265	0.070	3.55
1	6	1.50567	2.446456	-0.670607	-0.172941	0.070	3.55
1	6	-2.244765	1.840651	-0.557493	0.511584	0.070	3.55
2	7	-2.641177	0.540115	-0.474638	-0.558906	0.170	3.25
1	6	-1.623275	-0.327065	-0.225768	0.496432	0.070	3.55
4	5	-4.075551	0.140371	-0.389085	1.130301	0.095	3.54
5	8	-4.584662	-0.207829	-1.688693	-0.708028	0.170	3.07
1	6	-5.884035	-0.612796	-1.846975	0.474011	0.070	3.55
1	6	-6.21876	-1.965521	-1.760628	-0.228852	0.070	3.55
1	6	-7.531986	-2.372462	-1.961545	-0.125772	0.070	3.55
1	6	-8.555114	-1.459352	-2.254385	-0.109690	0.070	3.55
1	6	-8.195923	-0.111805	-2.34186	-0.114218	0.070	3.55
1	6	-6.882152	0.311246	-2.142166	-0.243745	0.070	3.55
2	7	-1.814002	-1.515645	0.361202	-0.581988	0.170	3.25
1	6	-3.02656	-1.767506	0.859067	0.478463	0.070	3.55
1	6	-3.43566	-2.667622	1.931297	-0.094464	0.070	3.55
1	6	-4.693238	-2.205008	2.407274	-0.001013	0.070	3.55
1	6	-5.041822	-1.027278	1.621189	0.363530	0.070	3.55
2	7	-4.092548	-0.941366	0.649862	-0.434141	0.170	3.25
1	6	-5.307755	-2.813214	3.501783	-0.091993	0.070	3.55
1	6	-4.670114	-3.896057	4.091537	-0.086632	0.070	3.55
1	6	-3.426683	-4.353531	3.621123	-0.080616	0.070	3.55
1	6	-2.791848	-3.739073	2.550337	-0.064599	0.070	3.55
2	7	-5.889108	-0.02885	1.891704	-0.537145	0.170	3.25
1	6	-5.667628	1.141637	1.284035	0.372602	0.070	3.55
2	7	-4.737211	1.294852	0.303131	-0.482006	0.170	3.25
1	6	-4.276693	2.574909	0.188462	0.505882	0.070	3.55
1	6	-5.180665	3.38776	0.994646	-0.107776	0.070	3.55
1	6	-6.048588	2.49296	1.678474	0.022993	0.070	3.55
1	6	-6.978168	2.96945	2.602802	-0.128495	0.070	3.55
1	6	-7.047926	4.339814	2.813092	-0.044725	0.070	3.55
1	6	-6.189203	5.224687	2.137673	-0.106283	0.070	3.55
1	6	-5.241272	4.760228	1.236011	-0.052890	0.070	3.55
2	7	-3.074239	2.863942	-0.311754	-0.600334	0.170	3.25
1	6	-9.990221	-1.958186	-2.468154	0.449143	0.070	3.55
1	6	-10.478356	-2.673615	-1.196773	-0.179315	0.066	3.50
1	6	14.294957	-1.878811	-0.02908	0.671754	0.105	3.75
5	8	15.100194	-1.155764	-0.823853	-0.566056	0.170	3.00
1	6	-10.96072	-0.813049	-2.775334	-0.177828	0.066	3.50
1	6	-10.020075	-2.943964	-3.648842	-0.124499	0.066	3.50
5	8	14.708809	-2.780221	0.665341	-0.553645	0.210	2.96
6	1	-2.951212	-5.203551	4.112895	0.098350	0.000	0.00
6	1	-1.818753	-4.080606	2.196531	0.095054	0.000	0.00
6	1	-6.262919	-2.444463	3.876458	0.104702	0.000	0.00
6	1	-4.562174	5.443552	0.725486	0.094044	0.000	0.00
6	1	-6.267404	6.295416	2.332249	0.102676	0.000	0.00
6	1	-7.629881	2.279356	3.13921	0.112173	0.000	0.00
6	1	1.238361	-0.937923	-0.147169	0.120946	0.000	0.00
6	1	2.28156	3.205168	-0.773607	0.115662	0.000	0.00
6	1	-0.123582	3.844646	-0.86866	0.108844	0.000	0.00
6	1	-5.436575	-2.694409	-1.542868	0.078987	0.000	0.00
6	1	-6.621585	1.367635	-2.223663	0.090076	0.000	0.00
6	1	-7.759035	-3.437617	-1.888433	0.129632	0.000	0.00
6	1	-8.946476	0.643191	-2.572156	0.109974	0.000	0.00
6	1	-11.973903	-1.216976	-2.920239	0.026458	0.000	0.00
6	1	-11.007524	-0.08457	-1.952138	0.020038	0.000	0.00
6	1	-10.682781	-0.275481	-3.694198	0.028497	0.000	0.00
6	1	-9.683937	-2.456196	-4.576669	-0.002906	0.000	0.00
6	1	-9.370759	-3.813548	-3.471055	0.010130	0.000	0.00
6	1	-11.043733	-3.317502	-3.810086	0.015621	0.000	0.00
6	1	-9.845241	-3.536993	-0.944911	0.010421	0.000	0.00
6	1	-10.47374	-1.989309	-0.334537	0.016160	0.000	0.00
6	1	-11.507017	-3.042138	-1.335983	0.036062	0.000	0.00
6	1	5.650828	-1.885537	-0.167334	0.137031	0.000	0.00
6	1	8.046107	-2.389826	-0.108073	0.120412	0.000	0.00
6	1	10.793757	0.781123	-1.589706	0.137339	0.000	0.00
6	1	9.887799	-2.295024	1.28476	0.120129	0.000	0.00
6	1	13.17627	0.124868	-1.533468	0.103301	0.000	0.00

```

6 1 12.283926 -2.944141 1.32851 0.101880 0.000 0.00
6 1 15.999483 -1.508992 -0.706029 0.424587 0.000 0.00
6 1 -5.136831 -4.399444 4.939574 0.102100 0.000 0.00
6 1 -7.77688 4.739901 3.519461 0.090867 0.000 0.00
6 104 4.267226 -0.6111025 -0.286279 0.000000 0.000 0.00
3 water TIP3P JCP 79, 926 1983
1 8 0.00000 0.117176 0.000000 -0.8340 0.1521 3.15061
2 1 0.75695 -0.468706 0.000000 0.4170 0.0000 0.00000
2 1 -0.75695 -0.468706 0.000000 0.4170 0.0000 0.00000
Send

```

Topology: subpc.dfr

```

$atoms fragments
1 1 58 6 90 5 88 4 7 3 87 2 89 R
2 7 4 8 86 9 85 10 69 16 11 26 15 35 14 36 13 37 12 R 44 43 63 42 92
3 16 10 94 17 18 19
4 28 29 27 F
5 29 28 30 72 31 74 32 56 33 75 34 73 R
6 56 57 60 61 32 R
7 57 56 83 82 84 R
8 58 59 1 62 F
9 59 58 91 F
10 60 56 77 76 78 R
11 61 56 80 81 79 R
Send atoms fragments

$fragment connection
1 8
1 2
2 3
3 4
4 5
5 6
6 11
6 10
6 7
8 9
Send fragment connection

$bond
1 6 0.0 0.0
1 2 0.0 0.0
2 89 0.0 0.0
2 3 0.0 0.0
3 87 0.0 0.0
3 4 0.0 0.0
4 7 0.0 0.0
4 5 0.0 0.0
5 88 0.0 0.0
5 6 0.0 0.0
6 90 0.0 0.0
7 12 0.0 0.0
7 8 0.0 0.0
8 86 0.0 0.0
8 9 0.0 0.0
9 85 0.0 0.0
9 10 0.0 0.0
10 16 0.0 0.0
10 11 0.0 0.0
11 15 0.0 0.0
11 12 0.0 0.0
12 13 0.0 0.0
13 14 0.0 0.0
14 15 0.0 0.0
16 94 0.0 0.0
16 17 0.0 0.0
17 18 0.0 0.0
18 23 0.0 0.0
18 19 0.0 0.0
19 69 0.0 0.0
19 20 0.0 0.0
20 26 0.0 0.0
20 21 0.0 0.0
21 24 0.0 0.0
21 22 0.0 0.0
22 71 0.0 0.0
22 23 0.0 0.0
23 70 0.0 0.0
24 55 0.0 0.0
24 25 0.0 0.0
25 27 0.0 0.0
25 26 0.0 0.0
26 35 0.0 0.0
27 47 0.0 0.0

```

```

27 40 0.0 0.0
29 34 0.0 0.0
29 30 0.0 0.0
30 72 0.0 0.0
30 31 0.0 0.0
31 74 0.0 0.0
31 32 0.0 0.0
32 56 0.0 0.0
32 33 0.0 0.0
33 75 0.0 0.0
33 34 0.0 0.0
34 73 0.0 0.0
35 36 0.0 0.0
36 40 0.0 0.0
36 37 0.0 0.0
37 44 0.0 0.0
37 38 0.0 0.0
38 41 0.0 0.0
38 39 0.0 0.0
39 45 0.0 0.0
39 40 0.0 0.0
41 65 0.0 0.0
41 42 0.0 0.0
42 92 0.0 0.0
42 43 0.0 0.0
43 63 0.0 0.0
43 44 0.0 0.0
44 64 0.0 0.0
45 46 0.0 0.0
46 50 0.0 0.0
46 47 0.0 0.0
47 48 0.0 0.0
48 55 0.0 0.0
48 49 0.0 0.0
49 54 0.0 0.0
49 50 0.0 0.0
50 51 0.0 0.0
51 68 0.0 0.0
51 52 0.0 0.0
52 93 0.0 0.0
52 53 0.0 0.0
53 67 0.0 0.0
53 54 0.0 0.0
54 66 0.0 0.0
56 61 0.0 0.0
56 60 0.0 0.0
56 57 0.0 0.0
57 84 0.0 0.0
57 83 0.0 0.0
57 82 0.0 0.0
60 78 0.0 0.0
60 77 0.0 0.0
60 76 0.0 0.0
61 81 0.0 0.0
61 80 0.0 0.0
61 79 0.0 0.0
1 58 400.0 1.485
27 28 450.0 2.500
28 29 450.0 1.370
58 62 570.0 1.210
58 59 450.0 1.343
59 91 553.0 0.973
$end bond

$angle
1 58 62 harmonic 80.0 124.54
1 58 59 harmonic 80.0 113.09
27 28 29 harmonic 80.0 102.20
58 59 91 harmonic 35.0 106.68
59 58 62 harmonic 80.0 122.37
$end angle

$dihedral
5 4 7 8 OPLS -0.025 1.163 0.00 0.0 0.0 0.0
5 4 7 12 OPLS -0.025 1.163 0.00 0.0 0.0 0.0
3 4 7 12 OPLS -0.025 1.163 0.00 0.0 0.0 0.0
3 4 7 8 OPLS -0.025 1.163 0.00 0.0 0.0 0.0
6 1 58 62 OPLS -0.200 4.350 0.00 0.0 0.0 0.0
6 1 58 59 OPLS 0.000 0.000 0.00 0.0 0.0 0.0
2 1 58 62 OPLS -0.200 4.350 0.00 0.0 0.0 0.0
2 1 58 59 OPLS 0.000 0.000 0.00 0.0 0.0 0.0
1 58 59 91 OPLS 0.000 4.830 0.00 0.0 0.0 0.0
62 58 59 91 OPLS 0.000 4.800 -3.00 0.0 0.0 0.0
9 10 16 94 OPLS 0.000 1.100 0.00 0.0 0.0 0.0
11 10 16 94 OPLS 0.000 0.00 0.00 0.0 0.0 0.0
25 27 28 29 OPLS -0.600 1.200 0.90 0.0 0.0 0.0
40 27 28 29 OPLS 0.000 0.000 0.00 0.0 0.0 0.0

```



```

47 27 28 29 OPLS    0.000    0.000  0.00  0.0    0.0  0.0
27 28 29 34 OPLS    0.000  -3.050    0.00  0.0    0.0    0.0
27 28 29 30 OPLS    0.000  -3.050    0.00  0.0    0.0    0.0
31 32 56 61 OPLS    0.000    80.000    0.00  0.0    0.0  0.0
31 32 56 60 OPLS    0.000    80.000    0.00  0.0    0.0    0.0
31 32 56 57 OPLS    0.000    80.000    0.00  0.0    0.0    0.0
33 32 56 61 OPLS    0.000    80.000    0.00  0.0    0.0    0.0
33 32 56 60 OPLS    0.000    80.000    0.00  0.0    0.0    0.0
33 32 56 57 OPLS    0.000    80.000    0.00  0.0    0.0    0.0
32 56 57 82 OPLS    0.0    0.0    0.46  0.0    0.0    0.0
32 56 57 83 OPLS    0.0    0.0    0.46  0.0    0.0    0.0
32 56 57 84 OPLS    0.0    0.0    0.46  0.0    0.0    0.0
60 56 57 82 OPLS    0.0    0.0    0.46  0.0    0.0    0.0
60 56 57 83 OPLS    0.0    0.0    0.46  0.0    0.0    0.0
60 56 57 84 OPLS    0.0    0.0    0.46  0.0    0.0    0.0
61 56 57 82 OPLS    0.0    0.0    0.46  0.0    0.0    0.0
61 56 57 83 OPLS    0.0    0.0    0.46  0.0    0.0    0.0
61 56 57 84 OPLS    0.0    0.0    0.46  0.0    0.0    0.0
32 56 60 76 OPLS    0.0    0.0    0.46  0.0    0.0    0.0
32 56 60 77 OPLS    0.0    0.0    0.46  0.0    0.0    0.0
32 56 60 78 OPLS    0.0    0.0    0.46  0.0    0.0    0.0
57 56 60 76 OPLS    0.0    0.0    0.46  0.0    0.0    0.0
57 56 60 77 OPLS    0.0    0.0    0.46  0.0    0.0    0.0
57 56 60 78 OPLS    0.0    0.0    0.46  0.0    0.0    0.0
61 56 60 76 OPLS    0.0    0.0    0.46  0.0    0.0    0.0
61 56 60 77 OPLS    0.0    0.0    0.46  0.0    0.0    0.0
61 56 60 78 OPLS    0.0    0.0    0.46  0.0    0.0    0.0
32 56 61 79 OPLS    0.0    0.0    0.46  0.0    0.0    0.0
32 56 61 80 OPLS    0.0    0.0    0.46  0.0    0.0    0.0
32 56 61 81 OPLS    0.0    0.0    0.46  0.0    0.0    0.0
57 56 61 79 OPLS    0.0    0.0    0.46  0.0    0.0    0.0
57 56 61 80 OPLS    0.0    0.0    0.46  0.0    0.0    0.0
57 56 61 81 OPLS    0.0    0.0    0.46  0.0    0.0    0.0
60 56 61 79 OPLS    0.0    0.0    0.46  0.0    0.0    0.0
60 56 61 80 OPLS    0.0    0.0    0.46  0.0    0.0    0.0
60 56 61 81 OPLS    0.0    0.0    0.46  0.0    0.0    0.0
$end dihedral

$improper dihedral
1 59 58 62    15.0    180.0
$end improper dihedral

```

---

DICE thermalization input: subpc.ter

---

```

title = subpc em agua
ljname = subpc-w.txt
outname = outsubpc-w
ncores = 8
init = yes
nmol = 1 2500
dens = 0.99
temp = 298.0
press = 1.0
upbuf = 150
accum = no
vstep = 0
nstep = 20000
iprint = 1
isave = 500
irdf = 0
iratio = 10
vratio = 10
seed = 366045
dielectric = 80.0
$end

```

---

DICE CBMC simulation input: subpc.in

---

```

title = subpc em agua
ljname = subpc-w.txt
outname = outsubpc-w
ncores = 8
init = no
press = 1.0
upbuf = 150
accum = no
vstep = 500000
nstep = 4
iprint = 1
isave = 50
irdf = 0
iratio = 10

```

```
vratio = 10
seed = 366045
sampling = 2
dielectric = 80.0
flex = subpc
equiphi = yes
ntrialphi = 32
fudge1j = 0.5
fudge1b = 0.5
pcbmc = 0.8
nsf = 10000
sfint = 1000
$end
```

---

## SI 5: References

- [1] Makoto Matsumoto and Takuji Nishimura. Mersenne twister: A 623-dimensionally equidistributed uniform pseudo-random number generator. In *ACM Transactions on Modeling and Computer Simulation*, volume 8, pages 3–30, 1998.
- [2] Mersenne Twister in FORTRAN. <http://www.math.sci.hiroshima-u.ac.jp/~m-mat/MT/VERSIONS/FORTRAN/fortran.html>. Accessed: 2020-03-25.
- [3] M. P. Allen and D. J. Tildesley. *Computer Simulation of Liquids, 2nd edition*. Oxford University Press, Oxford, 2017.
- [4] John C. Owicki. Optimization of Sampling Algorithms in Monte Carlo Calculations on Fluids. pages 159–171. jun 1978.
- [5] Bernard Bigot and William L. Jorgensen. Sampling methods for Monte Carlo simulations of n-butane in dilute solution. *J. Chem. Phys.*, 75(4):1944–1952, 1981.
- [6] William H. Press, Saul A. Teukolsky, William T. Vetterling, and Brian P. Flannery. *Numerical Recipes 3rd Edition: The Art of Scientific Computing*. Cambridge University Press, New York, 3rd edition, 2007.
- [7] Daan Frenkel and Berend Smit. *Understanding molecular simulation*. Academic Press, San Diego, 2nd edition, 2002.
- [8] William L. Jorgensen, David S. Maxwell, and Julian Tirado-Rives. Development and testing of the OPLS all-atom force field on conformational energetics and properties of organic liquids. *J. Am. Chem. Soc.*, 118(45):11225–11236, 1996.
- [9] Wendy D. Cornell, Piotr Cieplak, Christopher I. Bayly, Ian R. Gould, Kenneth M. Merz, David M. Ferguson, David C. Spellmeyer, Thomas Fox, James W. Caldwell, and Peter A. Kollman. A second generation force field for the simulation of proteins, nucleic acids, and organic molecules. *J. Am. Chem. Soc.*, 117(19):5179–5197, 1995.
- [10] J.A. Barker and R.O. Watts. Monte Carlo studies of the dielectric properties of water-like models. *Mol. Phys.*, 26(3):789–792, 1973.
- [11] Dominik Sidler, Simon Frasch, Michael Cristòfol-Clough, and Sereina Riniker. Anisotropic reaction field correction for long-range electrostatic interactions in molecular dynamics simulations. *J. Chem. Phys.*, 148(23):234105, 2018.
- [12] Sander Pronk, Szilárd Páll, Roland Schulz, Per Larsson, Pär Bjelkmar, Rossen Apostolov, Michael R. Shirts, Jeremy C. Smith, Peter M. Kasson, David VAN DER SPOEL, Berk Hess, and Erik Lindahl. Gromacs 4.5: a high-throughput and highly parallel open source molecular simulation toolkit. *Bioinf.*, 29(7):845–854, 2013.